Published online 13 January 2016

Nucleic Acids Research, 2016, Vol. 44, No. 3 ***1449–1470***
doi: 10.1093/nar/gkv1540

Selection-free gene repair after adenoviral vector transduction of designer nucleases: rescue of dystrophin synthesis in DMD muscle cell populations

Ignazio Maggio[1], Luca Stefanucci[1,2], Josephine M. Janssen[1], Jin Liu[1], Xiaoyu Chen[1], Vincent Mouly[3] and Manuel A.F.V. Gonçalves[1,*]

[1]Department of Molecular Cell Biology, Leiden University Medical Center, Leiden, Einthovenweg 20, 2333 ZC Leiden, The Netherlands, [2]Facoltà di Scienze Matematiche Fisiche e Naturali, Universitá di Roma Tor Vergata, Rome, Italy and [3]Center for Research in Myology, UMRS 974 UPMC-INSERM, FRE 3617 CNRS, Paris, France

Received July 27, 2015; Revised December 22, 2015; Accepted December 23, 2015

ABSTRACT

Duchenne muscular dystrophy (DMD) is a fatal X-linked muscle-wasting disorder caused by mutations in the 2.4 Mb dystrophin-encoding *DMD* gene. The integration of gene delivery and gene editing technologies based on viral vectors and sequence-specific designer nucleases, respectively, constitutes a potential therapeutic modality for permanently repairing defective *DMD* alleles in patient-derived myogenic cells. Therefore, we sought to investigate the feasibility of combining adenoviral vectors (AdVs) with CRISPR/Cas9 RNA-guided nucleases (RGNs) alone or together with transcriptional activator-like effector nucleases (TALENs), for endogenous *DMD* repair through non-homologous end-joining (NHEJ). The strategies tested involved; incorporating small insertions or deletions at out-of-frame sequences for reading frame resetting, splice acceptor knock-out for DNA-level exon skipping, and RGN-RGN or RGN-TALEN multiplexing for targeted exon(s) removal. We demonstrate that genome editing based on the activation and recruitment of the NHEJ DNA repair pathway after AdV delivery of designer nuclease genes, is a versatile and robust approach for repairing *DMD* mutations in bulk populations of patient-derived muscle progenitor cells (up to 37% of corrected *DMD* templates). These results open up a DNA-level genetic medicine strategy in which viral vector-mediated transient designer nuclease expression leads to permanent and regulated dystrophin synthesis from corrected native *DMD* alleles.

INTRODUCTION

Duchenne muscular dystrophy (DMD) is a severe X-linked inherited disease caused by mutations that disrupt the reading frame of the dystrophin-encoding *DMD* gene (1). The lack of functional dystrophin precludes the anchorage between cytoskeleton and sarcolemma structural components needed for the integrity of striated muscle tissue. This results in a cascade of events leading to progressive muscle degeneration and wasting followed by early death, typically between the third and fourth decade of life (2). The sheer size of *DMD* (∼2.4 Mb) combined with its mutational hotspots, regions linked to high rates of rearrangements and deletions, contribute to make DMD the most common muscular dystrophy in humans (∼1 in 3500 boys). Despite the identification in 1987 of the molecular basis responsible for DMD (1), to date there is no effective therapy available. Importantly, however, there is an increasing number of research lines based on molecular and cellular approaches aiming at tackling DMD (2,3).

Among the broad array of *DMD* mutations, the vast majority (>60%) comprises large intragenic deletions of one or more exons that disrupt the reading frame (4). In contrast, deletions within *DMD* yielding in-frame transcripts often result in the synthesis of shorter dystrophin forms that underlie milder Becker muscular dystrophy (BMD) phenotypes (2,3). This observation provided a strong rationale for developing therapeutic strategies based on delivering recombinant microdystrophins and antisense oligonucleotides (AONs) for gene replacement and exon skipping, respectively (3). In the latter approaches, disrupted *DMD* reading frames are restored at the RNA level by AON hybridization to specific splice site motifs in pre-mRNA templates with the consequent 'masking' of these motifs from the splicing machinery. This splicing interference avoids that exons disrupting the *DMD* reading frame are incorporated into mature mRNA transcripts. Therefore, similarly to microdystrophin delivery, the ultimate goal here is to convert

*To whom correspondence should be addressed. Tel: +31 71 5269238; Fax: +31 71 5268270; Email: M.Goncalves@lumc.nl

DMD into milder BMD forms (2,3). *DMD* transcript repair by exon skipping has entered clinical testing in the form of AONs targeting exon 51 (5,6). Despite initial indications of therapeutic benefit, the requirement for lifelong AON administrations and potential long-term AON toxicities, warrant the unabated pursuit of alternative or complementary DMD therapies. In addition, multi-exon skipping by AON multiplexing aiming at a wider mutant *DMD* genotype coverage remains rather inefficient (7).

Genome editing based on sequence-specific designer nucleases (also known as programmable nucleases) has recently been put forward as a potential therapeutic modality for restoring on a permanent basis the native *DMD* reading frame in patient-own cells, including stem and progenitor cells with myogenic capacity (8–12). The value of designer nucleases arises from their ability to induce site-specific double-stranded DNA breaks (DSBs) that stimulate the two main cellular DNA repair pathways, i.e. non-homologous end-joining (NHEJ) and homologous recombination (HR). The former pathway involves the direct end-to-end ligation of DNA termini created by chromosomal DSBs, often resulting in the introduction of small insertions and deletions (indels) at the junction; the latter requires 'homologous' donor DNA sequences to serve as templates for DNA synthesis-dependent DSB repair (13,14). Although extremely valuable to achieve precise endogenous gene repair and targeted addition of whole transgenes, current HR-based genome editing approaches are, to some extent, limited by the fact that DSBs are often repaired via NHEJ instead of HR (15). Moreover, the very large size of the *DMD* gene coupled to the broad distribution and types of its mutations, complicates the delivery of donor DNA substrates harboring the complete *DMD* coding sequence (11 kb) or mutation-correcting templates. Thus, the ligation of designer nuclease-induced chromosomal breaks by NHEJ provides for alternative, donor DNA-independent, approaches for repairing aberrant *DMD* reading frames. Importantly, such direct repair of native defective alleles assures the physiological regulation of dystrophin synthesis by keeping *DMD* expression under its endogenous promoter.

Designer nuclease technologies are developing at a rapid pace and include zinc-finger nucleases (ZFNs), engineered meganucleases, transcription activator-like effector nucleases (TALENs) and, more recently, RNA-guided nucleases (RGNs) (13,14). Among these, TALENs seem to display a particularly favorable specificity profile (16), whereas the RGN platform outstands for its simplicity and versatility, especially in multiplexing contexts (17). TALENs are modular proteins consisting of a DNA-binding domain (DBD) bearing repetitive motifs fused via a linker to a catalytic domain, commonly derived from the *FokI* endonuclease. These artificial proteins work in pairs with the binding of each monomer to its target site resulting in site-specific DSB formation after the *in situ* dimerization of the non-specific *FokI* nuclease domains (13,14). RGNs are in turn ribonucleoprotein complexes mostly based on the type II clustered, regularly interspaced, short palindromic repeat (CRISPR)-associated Cas9 (CRISPR−Cas9) nuclease system of *Streptococcus pyogenes*. These RGNs consist of Cas9 nuclease and chimeric single guide RNA (gRNA) moieties. The Cas9 protein is addressed via the 5′ portion of the gRNA to a 18–20 nucleotide-long complementary DNA sequence followed by a so-called protospacer adjacent motif (PAM; NGG in the case of *S. pyogenes* Cas9). After binding to the target site, a blunt-ended DSB is generated by Cas9 (13,14,17). Amongst other goals, this prokaryotic molecular immune system is being adapted as a powerful tool for the targeted genetic modification of human cells (17).

Proof-of-principle *DMD* reading frame correction experiments deploying designer nucleases have recently been carried out in human myoblasts and induced pluripotent stem cells (iPSCs) (9–12). However, in these studies, the suboptimal delivery of TALENs, ZFNs and RGNs into target cell populations required the pre-selection of individual *DMD* repaired clones or the reporter-assisted enrichment of target cell fractions exposed to nuclease activity. Hence, towards advancing the testing of DMD therapeutic protocols based on genome editing principles, it will be paramount devising improved systems for delivering designer nucleases into muscle cells and non-muscle cells with myogenic capacity. In this regard, designer nuclease-encoding adenoviral vectors (AdVs) constitute appealing *DMD* editing agents especially owing to their amenability to clinical-grade high-titer manufacture and straightforward cell tropism modifications (18,19). Concerning the latter aspect, work from our laboratory demonstrated that genetically retargeted AdV particles displaying apical fiber motifs from serotype 50 instead of those from prototypic serotype 5, bypass the absence of the coxsackievirus-adenovirus receptor (CAR) on the surface of therapeutically relevant cell types, including human muscle progenitor cells (20,21). Additional AdV traits directly relevant to genome editing efforts include their stringent episomal nature for transient designer nuclease expression, large cloning capacity for sizable *TALEN* and *Cas9* open reading frame (ORF) packaging, and high genetic stability for delivering intact *TALEN* ORFs containing highly repetitive tracts (22–24).

In this study, we sought to investigate the suitability of fiber-modified AdVs for the permanent restoration of *DMD* reading frames in patient-derived muscle cells upon transient expression of designer nucleases. These experiments entailed the use of patient-derived myoblasts harboring common intragenic deletions as target cells, and RGNs plus TALENs as designer nucleases. The NHEJ-mediated *DMD* repair strategies investigated were (i) incorporation of indels at out-of-frame sequences for reading frame resetting, (ii) DNA-level splicing disruption for permanent exon skipping and (iii) RGN-RGN and RGN-TALEN multiplexing for excision of reading frame-disrupting exons. We report that designer nuclease-encoding AdV particles are valuable *DMD* editing agents. Importantly, AdV transductions do not abolish the differentiation capacity of the gene-edited myoblasts ultimately resulting in direct, selection-free, detection of repaired *DMD* alleles and corresponding Becker-like proteins in bulk populations of differentiated muscle progenitor cells.

MATERIALS AND METHODS

Cells

Human embryonic kidney 293T cells and human cervix carcinoma HeLa cells (American Type Culture Collection)

were cultured in high-glucose Dulbecco's modified Eagle's medium (DMEM; Life Technologies) supplemented with 10% and 5% fetal bovine serum (FBS; Life Technologies), respectively, at 37°C in a humidified-air 10% CO_2 atmosphere. The *E1*-complementing AdV packaging cell line PER.C6 (25) was grown in Dulbecco's modified Eagle's medium (DMEM) supplemented with 10% fetal bovine serum (FBS) and 10 mM $MgCl_2$ (Sigma-Aldrich) at 37°C in a humidified-air 10% CO_2 atmosphere. The *E1*- and *E2A*-complementing AdV packaging cell line PER.E2A (26) was cultured in DMEM containing 10% FBS, 10 mM $MgCl_2$ (Sigma-Aldrich) and 250 mg/ml of Geneticin (Life Technologies). PER.E2A cells were regularly sub-cultured at 39°C and were shifted to 34°C for the proper folding of their *E2A*-encoded thermo-sensitive DNA-binding protein during AdV production and titration, as described elsewhere (27,28).

The origin of and culture conditions for the human myoblasts used in transduction experiments for validating the TALEN-encoding AdVs, have been previously described (29). The origin of and cultures conditions for the wild-type human myoblasts and for the DMD patient-derived myoblasts harboring *DMD* intragenic deletions Δ48–50 and Δ45–52, herein referred to as DMD.Δ48–50 and DMD.Δ45–52, respectively, have also been detailed elsewhere (30). These cells were immortalized through a combination of telomerase- and cyclin-dependent kinase 4-expressing vectors (30).

In brief, wild-type, DMD.Δ48–50 and DMD.Δ45–52 myoblasts were grown in Skeletal Muscle Cell Growth Medium (Ready-to-use, PromoCell). This medium was supplemented with 20% FBS, 1× Glutamax and 1× Penicillin/Streptomycin (all from Life Technologies). The various types of human myoblasts were kept at 37°C in a humidified-air 5% CO_2 atmosphere. Human myoblasts were shown to be mycoplasma-free.

RGN and TALEN design

The nucleotide sequences of gRNA candidates were identified by visual inspection of target regions searching for NGG PAM motifs or by using the CRISPRdirect algorithm (31). Subsequently, the gRNA candidate lists were shortened by further screening for potential off-target activity with the aid of the Cas-OFFinder algorithm (32). The selected gRNA sequences and respective PAM motifs are listed in Supplementary Table S1. The constructs coding for the *DMD* intron 43-specific TALEN pairs 12.TALEN-L/12.TALEN-R and 13.TALEN-L/13.TALEN-R were custom-designed (GeneArt, Life Technologies). The map and sequences of the various TALEN-encoding ORFs are shown in Supplementary Figure S1.

Plasmids

Standard recombinant DNA techniques were applied for the construction of the various lentiviral vector (LV) and AdV transfer plasmids (33). The complete and annotated DNA sequence of LV transfer plasmid AO58_pLKO.1-Blast::EGFP.U6.Dystuffer is presented in Supplementary Figure S2. This gRNA acceptor plasmid was constructed on the basis of pLKO.1-puro.U6.sgRNA.BfuAI.stuffer (Addgene plasmid #50920) (34) by inserting at the BclI recognition site, located between the two BveI (BfuAI isoschizomer) sites, a 3431-bp DNA fragment derived from the human dystrophin coding sequence. This stuffer DNA fragment harbors four additional BveI recognition sequences to increase the extent to which the plasmid is digested with this enzyme. In addition, AO58_pLKO.1-Blast::EGFP.U6.Dystuffer differs from pLKO.1-puro.U6.sgRNA.BfuAI.stuffer in that the human *PGK1* promoter drives the expression of a *Blast::EGFP* marker gene conferring green fluorescence and blasticidin resistance instead of puromycin resistance. The digestion of AO58_pLKO.1-Blast::EGFP.U6.Dystuffer with BveI generates CGGT and GTTT 5′ overhangs that can be directionally ligated to, respectively, the ACCG and AAAC 5′ overhangs of two annealed oligodeoxyribonucleotides corresponding to gRNA sequences. The resulting gRNA template, composed of guide and scaffold sequences, is under the transcriptionally control of the RNA polymerase III human U6 promoter and terminator sequences. For convenience, the various LV transfer plasmids derived from these cloning maneuvers are named according to the *DMD* target site of the gRNA they express, generically; pLV.gEn/In, where 'g' refers to gRNA, 'E' and 'I' refer to exon and intron, respectively, and 'n' indicates the corresponding exon or intron number. The sequences of all oligodeoxyribonucleotides deployed for assembling the different gRNA modules as well as their respective target sites are listed in Supplementary Table S1.

The construction of the AdV transfer plasmid pAdSh.PGK.Cas9 (Addgene plasmid #58253) and of its derivative AdV molecular clone $pAdV^{\Delta 2}$P.Cas9.F^{50} has been described before (23). The complete DNA sequences of the AdV transfer plasmids pAdShu.CMV.12.TALEN-L.IRES.DsRed, pAdShu.CMV.12.TALEN-R.IRES.DsRed, pAdShu.CMV.13.TALEN-L.IRES.DsRed and pAdShu.CMV.13.TALEN-R.IRES.DsRed are presented in Supplementary Figure S3. The full-length AdV molecular clones encoding the various TALENs were assembled via HR after the transformation of *E. coli* cells $BJ5183^{pAdEasy\text{-}1.50}$ (28) with the respective MssI-treated AdV transfer plasmids, as detailed elsewhere (27,28).

To generate the AdV transfer plasmids AT62_pAd.Shu.gE53.PGK.Cas9.SV40pA and AT64_pAd.Shu.gE51.2.PGK.Cas9.SV40pA, plasmids pLV.gE53 and pLV.gE51.2 were digested with *XhoI* (Thermo Scientific) and the resulting fragments, containing the *gE53* and *gE51.2* expression units, were isolated and ligated to the Eco147I-linearized plasmid backbone pAdSh.PGK.Cas9 (Addgene plasmid #58253) (23). These AdV transfer plasmids were used for the construction of the *E1*- and *E2A*-deleted fiber-modified AdV molecular clones AU10_$pAdV^{\Delta 2}$gE53.P.Cas9.F^{50} and AU12_$pAdV^{\Delta 2}$gE51.2.P.Cas9.F^{50}, according to the protocol detailed elsewhere (28).

Testing of gRNA-encoding LV transfer plasmids

Once cloned into LV acceptor plasmids, the sequence integrity of all gRNAs was assessed by Sanger sequencing. Functional assays were initiated by seeding 293T cells at a

density of 1.5×10^5 cells per well of 24-well plates (Greiner Bio-One). The next day, the cells were transfected with DNA mixtures consisting of 375 ng of hCas9 (Addgene plasmid #41815) (35) and 375 ng of each of the gRNA-expressing LV constructs. Positive controls were provided by co-transfecting hCas9 with a LV construct (pLV.POS) expressing a previously validated human *AAVS1*-specific gRNA, named AAVS1-T2 (35). Negative controls were provided by mock-transfected 293T cells or by 293T cells co-transfected with hCas9 and a LV acceptor construct expressing a non-targeting gRNA (pLV.NEG). The transfection plasmid mixtures were diluted in 50 μl of 150 mM NaCl (Merk), after which they received 3.3 μl of a 1 mg/ml polyethyleneimine solution (PEI, Polysciences) under vigorous shaking for about 10 s. After a 15-min incubation period at room temperature, the resulting linear polycation-plasmid DNA complexes were directly added to the culture medium of the test cells. After 7 h, the transfection mixtures were removed and fresh culture medium was added. The treated cell populations were kept in culture for 3 days, after which transfection efficiencies were assessed by flow cytometry, as described below. In parallel, total cellular DNA from mock-transfected and from plasmid-transfected cells was extracted by using the DNeasy Blood & Tissue Kit (Qiagen) according to the manufacturer's instructions. Finally, the frequencies of targeted chromosomal DSBs were assessed by T7 endonuclease I (T7EI)-based genotyping assays, as described below.

Validation of TALEN-encoding AdV transfer plasmids

PER.C6 cells were seeded at a density of 1.5×10^6 cells per well of 6-well plates (Greiner Bio-One). The next day, the cells were transfected with DNA mixtures consisting of 3 μg of pAdShu.CMV.12.TALEN-L.IRES.DsRed and 3 μg of pAdShu.CMV.12.TALEN-R.IRES.DsRed or 3 μg of pAdShu.CMV.13.TALEN-L.IRES.DsRed and 3 μg of pAdShu.CMV.13.TALEN-R.IRES.DsRed. Mock-transfected cells or cells transfected exclusively with 6 μg of pAdShu.CMV.12.TALEN-L.IRES.DsRed, served as negative controls. Each of the plasmid mixtures was diluted in 200 μl of 150 mM NaCl (Merck), after which they received 19.74 μl of a 1 mg/ml PEI solution under vigorous shaking for about 10 s. After a 15-min incubation period at room temperature, the resulting polycation–DNA complexes were directly added into the culture medium of the test cells. After an overnight incubation period, the transfection mixtures were removed and fresh culture medium was added. At 3 days post-transfection, total cellular DNA was isolated by organic solvent extractions and ethanol precipitations as previously described (36). Finally, the frequencies of targeted chromosomal DSBs were determined by deploying T7EI-based genotyping assays, as specified below.

LV production and titration

The LV transfer plasmids encoding validated gRNAs were used to generate the respective LV particle stocks. The procedures and reagents deployed for generating the vesicular stomatitis virus glycoprotein G (VSV-G)-pseudotyped LV preparations are detailed elsewhere (37,38). In brief, LV stocks were generated by transfecting 293T cells with each of the LV transfer plasmids mixed with the packaging construct psPAX2 (Addgene plasmid #12260) and the VSV-G pseudotyping construct pLP/VSVG (Life Technologies). At 3 days post-transfection, the cultured medium was collected and, after centrifugation steps, vector particle-containing supernatants were filtered through 0.45 μm pore-sized syringe filters (Pall) to remove remaining producer cell debris. The titration of the various gRNA- and Blast::EGFP-encoding LV preparations was initiated by applying limiting dilution series onto HeLa indicator cells seeded at a density of 5×10^4 cells per well of 24-well plates (Greiner Bio-One). At 3 days post-transduction, frequencies of transduced cells were determined by Blast::EGFP-directed flow cytometry as described below. The resulting functional vector particle titers corresponding to each LV batch are specified in Supplementary Table S2 as HeLa cell-transducing units per ml (HTU/ml).

Adenoviral vector production and characterization

The generation and characterization of the fiber-modified *E1*- and *E2A*-deleted AdVs $AdV^{\Delta 2}P.Cas9.F^{50}$ and $AdV^{\Delta 2}U6.gRNA^{S1}.F^{50}$ have been described before (23). The procedures to generate, purify and titrate the fiber-modified *E1*-deleted AdVs AdV.12.TALEN-L.F^{50}, AdV.12.TALEN-R.F^{50}, AdV.13.TALEN-L.F^{50} and AdV.13.TALEN-R.F^{50} have been described elsewhere (27,28). The titers of purified AdV batches AdV.12.TALEN-L.F^{50}, AdV.12.TALEN-R.F^{50}, AdV.13.TALEN-L.F^{50} and AdV.13.TALEN-R.F^{50} were 17.8×10^{10}, 5.62×10^{10}, 1.78×10^{10} and 10.0×10^{10} infectious units per ml (IU/ml), respectively.

The structural integrity of packaged AdV genomes was assessed by restriction fragment length analysis (RFLA) of DNA isolated from purified particles of AdV.12.TALEN-L.F^{50}, AdV.12.TALEN-R.F^{50}, AdV.13.TALEN-L.F^{50} and AdV.13.TALEN-R.F^{50}. The restriction enzymes BglII and XhoI were use in this analysis. The functional validation of TALEN-encoding AdVs was performed in human myoblasts as follows. Seventy thousand human myoblasts were seeded in 24-well plates. The next day, these cells were exposed in 500 μl to 1:1 mixtures of either AdV.12.TALEN-L.F^{50} and AdV.12.TALEN-R.F^{50} or AdV.13.TALEN-L.F^{50} and AdV.13.TALEN-R.F^{50}. The total multiplicities of infection (MOI) applied were 10 and 20 IU/cell. Mock-transduced cells served as negative controls. Three days post-transduction, total cellular DNA was isolated by using the DNeasy Blood & Tissue kit (Qiagen) according to the manufacturer's instructions, after which the detection of TALEN-induced DSBs was performed by using T7EI-based genotyping assays, as described below.

The generation and titration of the *E1*- and *E2A*-deleted fiber-modified AdVs $AdV^{\Delta 2}P.Cas9.gE53.F^{50}$ and $AdV^{\Delta 2}P.Cas9.gE51.2.F^{50}$ were performed as described before (23). The titers of purified stocks of $AdV^{\Delta 2}P.Cas9.gE53.F^{50}$ and $AdV^{\Delta 2}P.Cas9.gE51.2.F^{50}$ were 27.7×10^{10} and 13.9×10^{10} IU/ml, respectively. The structural integrity of packaged AdV genomes was assessed by RFLA of DNA isolated from purified particles of $AdV^{\Delta 2}P.Cas9.gE53.F^{50}$ and $AdV^{\Delta 2}P.Cas9.gE51.2.F^{50}$.

Transduction experiments

The generation of DMD patient-derived myoblasts stably expressing *DMD*-targeting gRNAs was carried out as follows. Myoblasts DMD.Δ48–50 and DMD.Δ45–52 were seeded in growth medium at a density of 4×10^4 cells per well of 24-well plates (Greiner Bio-One). The next day, the cells were exposed to a dose-range of the various gRNA- and Blast::EGFP-encoding LV preparations as indicated. After a 3-day incubation period, the inocula were removed and fresh culture medium was added onto the cells. After reaching confluence, transduction levels were determined, as described below, by Blast:EGFP-directed flow cytometry of target cell suspensions. Next, DMD.Δ48–50 and DMD.Δ45–52 myoblasts transduced with LV particles at the indicated MOIs, were selected for gene editing experiments. Prior to the initiation of these experiments, DMD.Δ48–50 and DMD.Δ45–52 myoblasts were cultured in the presence of 7.5 and 15 μg/ml of blasticidin (InvivoGen), respectively. Gene editing experiments started by seeding the resulting gRNA-expressing cells at a density of 4×10^4 cells per well of 24-well plates (Greiner Bio-One). The next day, the cells were exposed in 500-μl volumes to different MOIs of $AdV^{\Delta 2}$P.Cas9.F^{50}. Mock-transduced cells and, whenever indicated, cells lacking one or more components of individual or multiplexing nuclease complexes, served as negative controls. At three days post-transduction, genomic DNA was isolated by using the DNeasy Blood & Tissue kit (Qiagen), according to the manufacturer's instructions. The frequencies of targeted DSB formation were assessed via T7EI-based genotyping assays, as indicated below.

Long-term cultures of gene-edited DMD.Δ48–50 myoblasts were established as follows. First, DMD.Δ48–50 myoblasts stably transduced with LV.gE51.2 (herein referred to as DMD.Δ48–$50^{gE51.2}$), were seeded at a density of 4×10^4 cells per well of 24-well plates. Approximately 24 h later, the cells were incubated with $AdV^{\Delta 2}$P.Cas9.F^{50} at an MOI of 50 IU/cell in 500 μl of growth medium. Three days post-transduction, the inoculum was replaced with fresh growth medium and the cells were sub-cultured. At 3 and 31 days post-transduction, the frequencies of designer nuclease-induced indels were determined by T7EI -based genotyping assays, as described below.

Gene editing experiments with $AdV^{\Delta 2}$P.Cas9.gE53.F^{50} and $AdV^{\Delta 2}$P.Cas9.gE51.2.F^{50} were initiated by seeding DMD.Δ45–52 and DMD.Δ48–50 myoblasts, respectively, at a density of 3×10^4 cells per well of 24-well plates (Greiner Bio-One). The wells were pre-coated with a 0.1% (w/v) gelatin solution (Sigma-Aldrich). The next day, DMD.Δ45–52 and DMD.Δ48–50 myoblasts were exposed in 500-μl volumes to the indicated MOIs of $AdV^{\Delta 2}$P.Cas9.gE53.F^{50} and $AdV^{\Delta 2}$P.Cas9.gE51.2.F^{50}, respectively. Mock-transduced cells served as negative controls. Three days post-transduction, genomic DNA was isolated and the frequencies of targeted DSB formation were assessed by using T7EI-based genotyping assays or by performing TIDE analysis as indicated below.

Flow cytometry

The percentages of Blast::EGFP-positive cells were determined by using a BD LSR II flow cytometer (BD Biosciences). Mock-transfected or mock-transduced target cells were used to set background fluorescence levels. At least 10 000 viable single cells were analyzed per sample. Data were analyzed with the aid of FlowJo 7.2.2 software (Tree Star).

Indel detection by T7EI-based genotyping assays

Targeted DSB formation was assessed by using the mismatch-sensing T7EI enzyme. To this end, genomic DNA samples from transfected or transduced cells were subjected to PCR for amplifying DNA segments encompassing the target sites of the different designer nucleases. The primer sequences, the PCR mixture compositions and the cycling parameters are specified in the Supplementary Tables S3 and S4. The PCR amplifications were performed by using GoTaq® G2 Flexi DNA Polymerase (Promega). Subsequently, the resulting amplicons were denaturated and slowly re-annealed by applying the program indicated in Supplementary Table S5. Next, one-fifth of each PCR mixture was incubated in 15-μl reactions with 1× NEBuffer 2 and 5 U of T7EI (both from New England Biolabs). After 15 min. at 37°C, the samples were subjected to electrophoresis through 2% (w/v) agarose gels in 1× Tris–acetate–EDTA (TAE) buffer. The resulting ethidium bromide-stained DNA species were detected by using a Molecular Imager Gel-Doc™ XR+ (Bio-Rad) and the proportion of digested amplicon products were determined by densitometry using Image Lab 4.1 software (Bio-Rad). Finally, the fraction of designer nuclease-targeted alleles were calculated by applying the following formula: $100 \times [1 - (1 - \text{fraction cleaved})^{1/2}]$ (39).

Indel detection by Tracking of Indels by DEcomposition (TIDE) analysis

PCR mixtures containing amplicons spanning RGN target sequences were purified using SureClean Plus (Bioline) according to the manufacturer's recommendations. Next, the purified PCR amplicons were subjected to Sanger sequencing (BaseClear, Leiden, the Netherlands). The indel spectra were obtained through the online TIDE tool (http://tide.nki.nl) (40) by using as input the PCR product chromatograms derived from edited and unedited DNA as indicated. The indel size ranges were set to 20 nucleotides upstream and downstream of the RGN target sequences.

Off-target analysis

The Cas-OFFinder algorithm (32) was used to select potential off-target sites of gE53:Cas9 and gE51.2:Cas9 complexes. Genomic DNA samples were extracted from DMD.Δ45–52 and DMD.Δ48–50 myoblasts transduced, respectively, with $AdV^{\Delta 2}$P.Cas9.gE53.F^{50} and $AdV^{\Delta 2}$P.Cas9.gE51.2.F^{50} at an MOI of 100 IU/cell. Genomic DNA extracted from mock-transduced DMD.Δ45–52 and DMD.Δ48–50 myoblasts served as negative controls. Next, genomic segments encompassing the indicated off-target sites were subjected to PCR amplifications with the respective composition, cycling parameters and primers being listed in Supplementary Tables S3 and

S4. Finally, indel detection was assessed by T7EI-based genotyping assays according the above-described protocol.

Detection of designer nuclease-induced *DMD* deletions

Two-μl genomic DNA samples from mock- or AdV-transduced cells were subjected to PCR for amplifying DNA fragments flanking the designer nuclease target sites. The primer sequences, PCR mixture compositions and cycling parameters are indicated in the Supplementary Tables S3 and S4. The detection of the resulting PCR products was performed by conventional agarose gel electrophoresis in 1× TAE buffer.

DMD mRNA expression analysis

DMD myoblasts were seeded in 24-well plates (Greiner bio-one) pre-coated with a 0.1% (w/v) gelatin solution (Sigma-Aldrich). The next day, the cells were incubated with designer nuclease-encoding AdV particles as described earlier. Three days post-transduction, the inocula were discarded and the cells were exposed to mitogen-poor conditions to induce differentiation leading to cell–cell fusion and myotube formation. To this end, the growth medium was replaced by phenol red-free DMEM supplemented with 0.05% bovine serum albumin (Sigma-Aldrich), 10 ng/ml epidermal growth factor (Sigma-Aldrich), 1 mM creatine monohydrate (Sigma-Aldrich), 50 μg/ml uridine (Sigma-Aldrich), 100 ng/ml pyruvic acid (Sigma-Aldrich), 1× Penicillin/Streptomycin (Life Technologies) and 1× GlutaMax (Life Technologies).

After myoblast differentiation (typically after 5- to 7-days in differentiation medium), the resulting myotubes were collected after adding 350 μl of buffer RA1 (Macherey-Nagel) and 3.5 μl ß-mercaptoethanol (Merck). The total RNA was extracted by using the NucleoSpin RNA II kit (Macherey-Nagel), according to the manufacturer's instructions. Reverse transcription of 1 μg of total RNA was carried out at 50°C for 1 h by using 200 ng of random primers, 0.2 mM dNTPs, 1× First-Strand Buffer, 5 mM dithiothreitol, and 200 U of SuperScript III Reverse Transcriptase (all from Life Technologies). Subsequently, 2 μl of the resulting cDNA molecules were used for PCR amplifications with primers annealing to exons 43 and 55, i.e. flanking the major *DMD* mutational hotspot in the X chromosome. The corresponding primer sequences, PCR mixture compositions and cycling parameters are listed in Supplementary Tables S3 and S4. The resulting PCR products were next subjected to electrophoresis through 1.2% (w/v) agarose gels in 1× TAE buffer.

Sanger DNA sequencing

PCR and RT-PCR products corresponding to mock- or AdV-transduced myoblasts were purified by using the JETquick Gel Extraction Spin kit (Genomed), according to the manufacturer's recommendations and were ligated to the pJET1.2/blunt backbone using the CloneJET PCR cloning Kit (Thermo Scientific). Next, chemically-competent cells of *E. coli* strain DH5α were transformed with the products of ligation. After overnight incubation at 30°C, randomly-selected clones were grown in 2.5 ml of Luria Broth medium supplemented with 100 μg/ml Ampicillin (MP Biomedical). Plasmids were extracted by using the JETquick Plasmid Miniprep Spin kit (Genomed) following the protocol provided by the manufacturer. Transformants were screened by PCR or by RFLA deploying XhoI and NcoI (both from Thermo Scientific). The selected inserts were subjected to Sanger sequencing (BaseClear, Leiden, the Netherlands) with the alignment of the resulting sequence reads being performed with the aid of AlignX, Vector NTI Advance® 11.5.0 software.

Immunofluorescence microscopy

Wild-type myoblasts and DMD.Δ48–50$^{gE51.2}$ myoblasts were seeded at a density of 3.5×10^4 cells per well of 24-well plates (Greiner bio-one). The wells were pre-coated with a 0.1% (w/v) gelatin solution (Sigma-Aldrich). The next day, the DMD.Δ48–50$^{gE51.2}$ myoblasts were exposed in 500-μl volumes to AdV$^{\Delta2}$P.Cas9.F^{50} or to AdV$^{\Delta2}$U6.gRNA^{S1}.F^{50} at 50 IU/cell. Mock-transduced wild-type myoblasts served as positive controls. Three days post-transduction, myoblast differentiation and fusion were triggered by adding mitogen-poor medium (see above). After differentiation, the myotube-containing cultures were washed twice with PBS for 5 min and fixed with 4% (v/v) paraformaldehyde in PBS for 30 min at room temperature. The fixative was removed by three 5-min washes with 10 mM glycine in PBS (PBSG). Next, the cells were permeabilized by adding 0.1% (w/v) Triton X-100 in PBS for 5 min at room temperature. The detergent was removed by three 5-min washes with PBSG. Next, a blocking step was performed by incubating the cells for 2 h with PBSG containing 5% FBS (Life Technologies). A rabbit polyclonal antibody directed against the C-terminus of dystrophin (ab15277; abcam) was diluted 1:100 in PBSG with 5% FBS. After an overnight incubation period at 4°C, the cells were rinsed three times with PBS and stained with an Alexa Fluor 568 anti-rabbit IgG1 secondary antibody (Life Technologies) diluted 1:1000 in PBSG containing 5% FBS. After incubation for 2 h at 4°C, excess secondary antibody was removed by four washes with PBS and two washes with Milli-Q water (MilliPore). Air-dried specimens were subsequently exposed to a drop of ProLong Gold Antifade Mountant containing 4′,6-diamidino-2-phenylindole (Life Technologies) and covered with a glass cover slide. Digital images were acquired by using an Olympus IX51 inverse fluorescence microscope, a XC30 Peltier CCD camera and CellF software (all from Olympus).

Wild-type myoblasts and DMD.Δ48–50 myoblasts were seeded at a density of 3×10^4 cells per well of 24-well plates (Greiner bio-one). The wells were pre-coated with a 0.1% (w/v) gelatin solution (Sigma-Aldrich). The next day, the DMD.Δ48–50 myoblasts were exposed to AdV$^{\Delta2}$P.Cas9.gE51.2.F^{50} at 12.5 IU/cell in 500 μl. Mock-transduced wild-type myoblasts served as positive controls. Three days post-transduction, myoblasts were triggered to differentiate by exposing them to mitogen-poor medium (see above). After incubation for 5 days in differentiation medium, the myotube-containing cultures were stained as described above, except for the following variations. The aforementioned primary antibody directed against dys-

trophin (ab15277; abcam) was incubated overnight together with the NCL-b-DG mouse monoclonal antibody directed against β-dystroglycan (clone 43DAG1/8D5, Novocastra). The dystrophin- and β-dystroglycan-specific antibodies were diluted 100- and 50-fold, respectively, in PBSG with 5% FBS. Secondary antibodies Alexa Fluor 568 anti-rabbit IgG (H+L; Life technologies) and Alexa Fluor 488 anti-Mouse IgG (H+L; Invitrogen) were diluted 1:500 in PBSG with 5% FBS. Cell nuclei were stained with Hoechst 33342 (Molecular Probes) diluted 1:1000 in PBS for 10 min in the dark, after which the DNA dye was removed by four washes with PBS. Digital images were acquired by using an AF6000 LX system and LAS AF software version 2.7.4.10100 (both from Leica). The merging of fluorescence signals was done by using Adobe Photoshop CS6 software (version 13.0 x64).

Western blot analysis

Western blotting was performed on DMD.Δ48–50$^{gE51.2}$ myotubes differentiated from progenitors that had been transduced with AdV$^{\Delta 2}$P.Cas9.F^{50} at an MOI of 50 IU/cell. Differentiated mock-transduced wild-type myoblasts served as a positive control; differentiated mock-transduced DMD.Δ48–50$^{gE51.2}$ myoblasts and undifferentiated wild-type myoblasts provided for negative controls. Myotubes present in wells of 24-well plates were lysed by incubation on ice for 30 min in 50 μl of RIPA buffer (Thermo Scientific) supplemented with a protease inhibitor cocktail (cOmplete^{TM} Mini, Sigma-Aldrich). Protein concentrations were determined by using a bicinchoninic acid assay (BCA, Thermo Scientific) according to the manufacturer's instructions; absorption was measured at $\lambda = 562$ nm with a Precisely 1420 multilabel counter (PerkinElmer). Next, the cell lysates were diluted in 4× sample buffer and 20× reducing agent (both from Bio-rad) and incubated at 95°C for 5 min. Protein samples (18.5 μg each) and 15 μl of HiMark^{TM} Prestained Protein Standard (Thermo Scientific) were loaded in a 3–8% Criterion^{TM} XT Tris-Acetate precast gel (Bio-Rad). The gel was placed on an ice-cooled Criterion^{TM} Cell and was run in XT Tricine running buffer (both from Bio-Rad) first for 1 h at 75 V (0.07 A) and then for 2.5 h at 150 V (0.12 A). Subsequently, the resolved proteins were transferred with the aid of a Trans-Blot® Turbo^{TM} Midi nitrocellulose pack and a Trans-Blot Turbo^{TM} system (both from Bio-Rad), according to the manufacturer's recommendation for high molecular weight proteins (2.5 A, 25 V, 10 min). The nitrocellulose membrane was blocked in Tris-buffered saline (TBS, Thermo Scientific) containing 5% nonfat dried milk (Elk; Campina Melkunie), washed in TBS with 0,05% (v/v) Tween 20 (TBST, Thermo Scientific) and incubated with a rabbit polyclonal antibody directed against dystrophin (ab15277; abcam) diluted in TBS. After an overnight incubation period at 4°C, the membrane was washed in TBST and was incubated for 4 h at 4°C with an anti-rabbit IgG secondary antibody conjugated to horseradish peroxidase (IgG-HRP; Santa Cruz) diluted in TBS. Proteins were detected by using horseradish peroxidase substrate Pierce^{TM} ECL2 (Thermo Scientific) following the manufacturer's specifications with the aid of Super RX-N X-Ray film (Fujifilm).

DMD.Δ45–52 and DMD.Δ48–50 myotubes differentiated from progenitors transduced with AdV$^{\Delta 2}$P.Cas9.gE53.F^{50} and AdV$^{\Delta 2}$P.Cas9.gE51.2.F^{50}, respectively, were obtained as described before (Transduction experiments). Mock-transduced wild-type myoblasts served as positive controls. Western blot analysis was carried out essentially as above-described except for the following differences: (i) quantification of protein amounts by BCA was substituted by incorporating tubulin as an internal loading control antigen; (ii) the proteins were blotted onto PVDF membrane (Trans-Blot® Turbo^{TM} Midi PVDF pack, Bio-Rad) and (iii) the blocking and antibody dilutions were done by using Blocker^{TM} Blotto in TBS (Thermo Scientific). The primary antibodies used were a rabbit polyclonal directed against dystrophin (ab15277; abcam), a mouse monoclonal specific for sarcomeric α-actinin (Sarcomeric, A7811; Sigma-Aldrich) and a rabbit polyclonal directed against α/β Tubulin (CST #2148).

RESULTS

DMD repair strategies based on AdV delivery of designer nucleases

Over 60% of *DMD* mutations correspond to intragenic deletions of one or more exons (4) leading to the disruption of the correct *DMD* reading frame (Supplementary Figure S4). We started by designing different NHEJ-mediated *DMD* editing strategies based on AdV transduction of sequence-specific engineered nucleases. To this end, we made use of DMD patient-derived myoblasts lacking exons 48 through 50 (DMD.Δ48–50) or exons 45 through 52 (DMD.Δ45–52) (30). The *DMD* genotypes Δ48–50 and Δ45–52 yield out-of-frame mRNA transcripts carrying premature stop codons within exon 51 and exon 53, respectively. As a result, the levels of dystrophin are undetectable in these cells. To investigate the use of designer nuclease-encoding AdV particles for proper *DMD* reading frame restoration in DMD.Δ48–50 myoblasts, we targeted genomic sequences located between the SA of exon 51 and the premature stop codon in the same exon. A fraction of the resulting chromosomal DNA junctions formed by NHEJ-mediated DSB repair is expected to contain indel footprints that correct the *DMD* reading frame either through frame-shifting or, in case of SA knockout, exon-skipping (Figure 1A). Likewise, in DMD.Δ45–52 myoblasts, in-frame mRNA transcripts are expected to be formed after site-specific DSB formation at genomic sequences positioned between the SA of exon 53 and the premature stop codon in this exon (Figure 1B).

We also tested AdV-mediated *DMD* repair in DMD.Δ45–52 myoblasts by triggering NHEJ-mediated exon 53 excisions. This maneuver is expected to rescue dystrophin synthesis as splicing of exon 44 to exon 54 generates an in-frame mRNA species (Figure 2A). In these experiments, multiplexing pairs of RGN complexes targeting sequences flanking exon 53 were used. Finally, in order to broaden the theoretical applicability of AdV-mediated *DMD* repair approaches based on targeted chromosomal DNA deletions, we also tested multiplexing RGN-RGN and RGN-TALEN pairs to remove the over 500 kb-long major *DMD* mutational hotspot region (Figure 2B). In

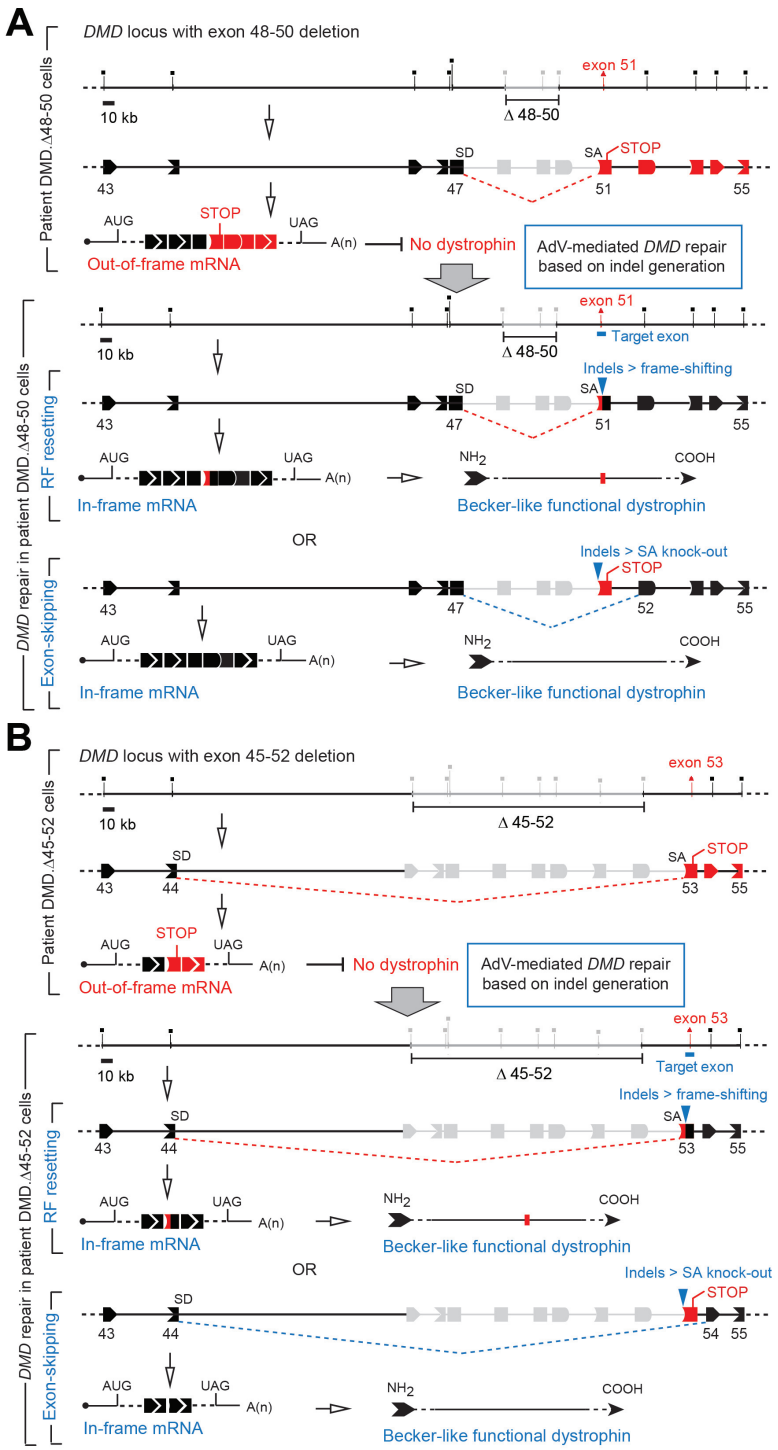

Figure 1. Gene editing strategies based on AdV delivery of designer nucleases for *DMD* repair by NHEJ-mediated indel formation. (**A**) *DMD* repair through targeted DSB-induced indel formation in DMD.Δ48–50 muscle cells. *DMD* deletions encompassing exons 48 through 50 yield mRNA transcripts whose sequences are frame-shifted downstream of the junction formed between exons 47 and 51. These out-of-frame mRNA templates lead to low or no dystrophin synthesis in differentiated muscle cells. In DMD.Δ48–50 muscle cells, the formation of targeted DSBs at sequences located between the splice acceptor (SA) site of exon 51 and the premature stop codon present in the same exon can yield NHEJ-derived indels that restore the proper *DMD* reading frame either through reading frame (RF) resetting or SA knockout-mediated exon-skipping. The expected outcome is the production of functional, albeit shorter, Becker-like dystrophin proteins. stop, premature stop codon; SD, splice donor. (**B**) *DMD* repair through targeted DSB-induced indel formation in DMD.Δ45–52 muscle cells. *DMD* deletions spanning exons 45 through 52 result in mRNA transcripts whose sequences are frame-shifted downstream of the junction generated between exons 44 and 53. These out-of-frame mRNA molecules result in low or no dystrophin synthesis. In patient DMD.Δ45–52 muscle cells, the generation of site-specific DSBs at sequences present between the SA of exon 53 and the premature stop codon located in the same exon can result in NHEJ-derived indels which restore the correct *DMD* reading frame either via RF resetting or SA knockout-mediated exon-skipping. The expected outcome is the synthesis of functional, albeit shorter, Becker-like dystrophin proteins.

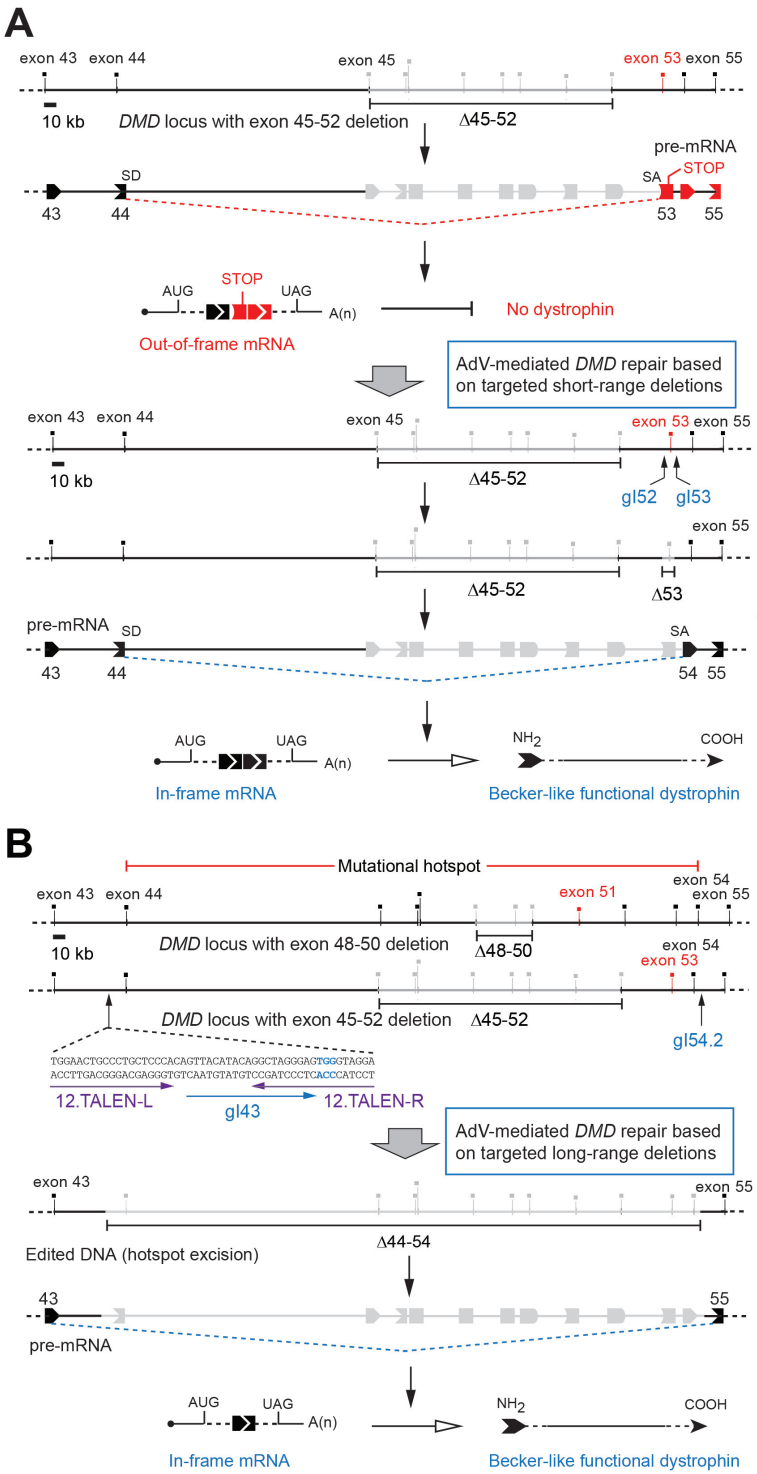

Figure 2. Gene editing strategies based on AdV delivery of designer nuclease pairs for *DMD* repair by NHEJ-mediated exon deletions. (**A**) *DMD* repair through short-range, single exon, deletion in DMD.Δ45–52 muscle cells. *DMD* deletions encompassing exons 45 through 52 lead to mRNA transcripts whose sequences are frame-shifted downstream of the junction formed between exons 44 and 53. These out-of-frame mRNA templates lead to reduced or undetectable levels of dystrophin in muscle cells. In patient DMD.Δ45–52 muscle cells, the NHEJ-mediated removal of exon 53 by RGN multiplexing with the indicated intron-specific gRNAs is expected to rescue dystrophin synthesis as splicing of exon 44 to exon 54 assembles an in-frame mRNA species. stop, premature stop codon; SD, splice donor; SA, splice acceptor. (**B**) *DMD* repair via long-range, multi exon, deletion in DMD.Δ48–50 and DMD.Δ45–52 muscle cells. Approximately 60% of *DMD* mutations map within a major mutational hotspot spanning exons 45 through 53. These mutations can, in principle, all be tackled by gene editing strategies based on NHEJ-mediated deletions covering the mutation-prone hotspot region as joining of exon 43 to exon 55 yields in-frame mRNA transcripts. Although internally truncated, this transcript is expected to yield a functional dystrophin protein. Targeted DSB-induced deletion of the large *DMD* mutational hotspot was tested by using AdV-mediated delivery of designer nuclease pairs whose members consist of RGN complexes (Cas9:gI43/Cas9:gI54.2) or of an RGN complex (Cas9:gI54.2) combined with a TALEN dimer (12.TALEN-L/12.TALEN-R).

common, the various strategies aim at generating in-frame mRNA transcripts from defective *DMD* loci which are then translated into functional, albeit shorter, Becker-like dystrophin proteins. Importantly, fiber-modified AdV particles were used in all *DMD* editing experiments to circumvent the absence of CAR on the surface of human myoblasts (20,21) and hence maximize designer nuclease gene delivery for direct, selection-free, restoration of *DMD* expression in target cell populations.

Construction and screening of gRNAs targeting *DMD*

To evaluate the various NHEJ-mediated *DMD* repair strategies based on AdV delivery of RGN components, we constructed and tested a panel of gRNAs targeting various intronic and exonic *DMD* sequences (Supplementary Table S1). As presented in the overview of the experimental workflow utilized in this study (Supplementary Figure S5), expression units encoding gRNA candidates were assembled in the context of LV transfer plasmids. The DNA cleaving activity conferred by each gRNA was assessed by co-transfecting 293T cells with gRNA- and Cas9-encoding plasmids and carrying out T7EI-based genotyping assays for determining indel frequencies after site-specific DSB repair. These assays showed that out of the 13 gRNAs assembled, 11 were able to generate relatively high frequencies of NHEJ-derived indels at the intended target sequences (Supplementary Figure S6). These frequencies varied from a minimum of 7% to a maximum of 53% of modified alleles in the transfected cell fractions (Supplementary Figures S6, panel C). Next, LV plasmids encoding functional gRNAs were selected for generating LV particles, which were in turn used to establishing cultures of DMD myoblasts expressing gRNAs. These target cells (Supplementary Figure S7) were subsequently used in the gene editing experiments described next.

AdV-mediated *DMD* repair based on targeted indel formation

Cultures of DMD.Δ48–50$^{gE51.2}$, DMD.Δ45–52^{gE53} and DMD.Δ45–52^{gNEG} myoblasts were established by LV transduction and blasticidin selection (Supplementary Figure S5). Next, they were either mock-transduced or were transduced with AdV$^{\Delta 2}$P.Cas9.F^{50} (23) at MOIs ranging from 25 through 200 IU/cell. T7EI-based genotyping assays revealed that indel frequencies in DMD.Δ48–50$^{gE51.2}$ and DMD.Δ45–52^{gE53} varied from a minimum of 8% to a maximum of 53% (Figure 3). As expected, DMD myoblats not exposed to AdV$^{\Delta 2}$P.Cas9.F^{50} or exposed to AdV$^{\Delta 2}$P.Cas9.F^{50} but expressing a non-targeting gRNA instead (gNEG), did not contain indels at detectable levels (Figure 3). The RGN-dependent *DMD* sequence modifications detected in human myoblasts were further confirmed by sequencing randomly selected molecular clones containing amplicons spanning the target sites for each RGN complex (i.e. gE51.2:Cas9 and gE53:Cas9) (Supplementary Figure S8). Of note, all clones analyzed had the SA dinucleotide AG intact.

After establishing robust NHEJ-mediated *DMD* editing by using AdV transduction of Cas9, we investigated whether gene-edited cells are stably maintained in the population. Therefore, DMD.Δ48–50$^{gE51.2}$ myoblasts that had been exposed to AdV$^{\Delta 2}$.Cas9.F^{50} at an MOI of 50 IU/cell were subjected to sub-culturing. As assessed by T7EI-based genotyping assays, the frequencies of gene editing events were similar at early and late time points post-transduction indicating the absence of a growth advantage in favor of unmodified cells (Supplementary Figure S9).

As transduction of DMD.Δ48–50$^{gE51.2}$ and DMD.Δ45–52^{gE53} myoblasts with AdV$^{\Delta 2}$P.Cas9.F^{50} prevented neither their differentiation nor their fusion capacities, we sought to investigate the rescue of proper *DMD* expression in these cells. RT-PCR analysis of *DMD* transcripts isolated from differentiated wild-type and DMD.Δ48–50$^{gE51.2}$ myoblasts yielded amplicons whose sizes were consistent with their respective genotypes (Figure 4A). Importantly, RT-PCR analysis of *DMD* transcripts extracted from differentiated DMD.Δ48–50$^{gE51.2}$ progenitors that had been transduced with AdV$^{\Delta 2}$P.Cas9.F^{50} led to the detection of additional transcripts. Sanger sequencing demonstrated that the higher molecular weight species present in these cells correspond to a mixture of unmodified and indel-containing mRNA templates, whereas the lower molecular weight form is derived exclusively from mRNA templates lacking exon 51. Similarly, RT-PCR analysis of differentiated DMD.Δ45–52^{gE53} progenitors initially transduced with AdV$^{\Delta 2}$P.Cas9.F^{50} led, in addition to unmodified templates, to the detection of new mRNA species containing either indels or, in this case, the deletion of exon 53 (Figure 4B). The mRNA templates lacking either exon 51 or exon 53 are likely to have been assembled through a DNA-level exon skipping mechanism in which indel formation knocked-out key *cis*-acting splicing elements. Of note, the asterisks marking the position of the intermediate-sized DNA species indicated in Figure 4, as well as elsewhere in this study, correspond to heteroduplexes formed during PCR by the hybridization of the upper and lower DNA fragments (Supplementary Figure S10).

To complement the analysis of gene expression from repaired *DMD* alleles, immunofluorescence microscopy was carried out on differentiated DMD.Δ48–50$^{gE51.2}$ myoblast populations initially transduced either with AdV$^{\Delta 2}$P.Cas9.F^{50} or with control vector AdV$^{\Delta 2}$U6.gRNA^{S1}.F^{50} (Figure 5A). In addition, the emergence of Becker-like dystrophin molecules after transduction of DMD.Δ48–50$^{gE51.2}$ myoblasts with AdV$^{\Delta 2}$P.Cas9.F^{50} was established by western blot analysis (Figure 5B). The detection of dystrophin protein in gene-edited DMD.Δ48–50$^{gE51.2}$ myotubes confirms that AdV and RGN technologies can be tailored for rescuing *DMD* expression without needing to resort to clonal isolation or experimental expedients to select the cell fractions that have taken-up the nuclease (Figure 5).

AdV-mediated *DMD* repair based on short-range targeted DNA deletions

Transduction of gRNA-expressing myoblasts DMD.Δ45–52^{gI52} and DMD.Δ45–52^{gI53} with AdV$^{\Delta 2}$P.Cas9.F^{50} (Supplementary Figure S11A) readily led to the detection of DSBs at the corresponding target sites (Supplementary

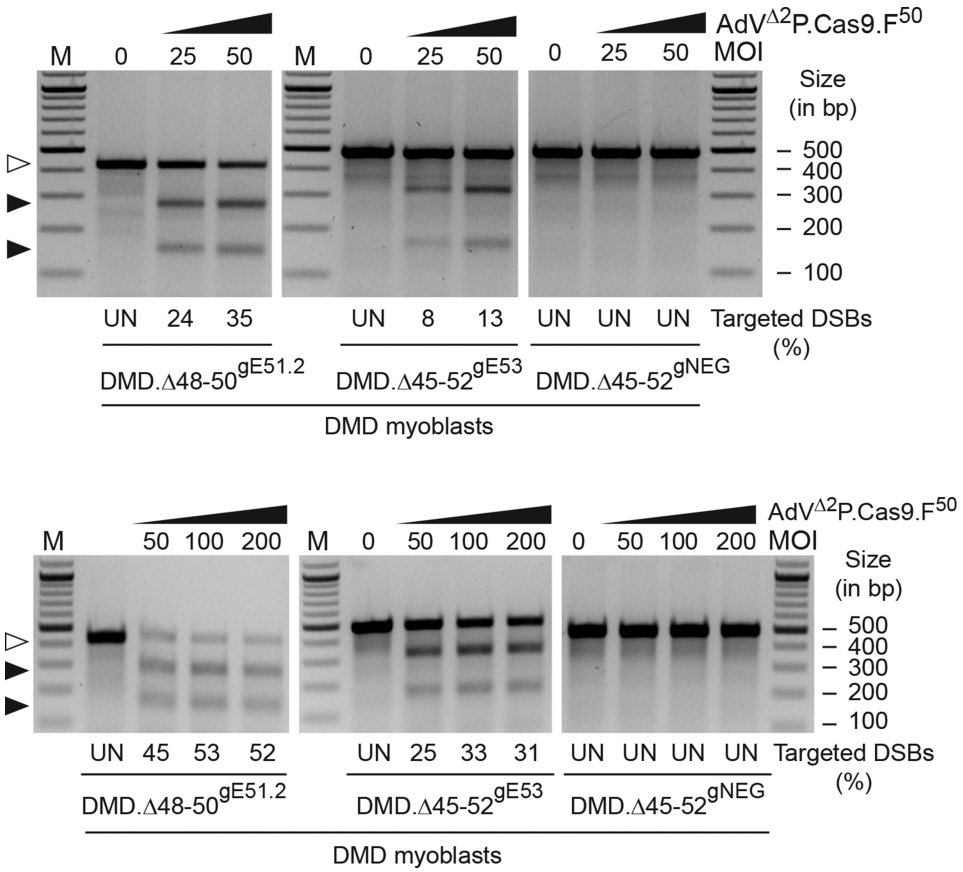

Figure 3. Testing gRNAs designed for NHEJ-mediated indel formation in human myoblasts transduced with Cas9-encoding AdV particles. Myoblasts DMD.Δ48–50 and DMD.Δ45–52 expressing gRNAs gE51.2 and gE53 (DMD.Δ48–50$^{gE51.2}$ and DMD.Δ45–52^{gE53}, respectively), were either mock-transduced or were transduced with AdV$^{\Delta 2}$P.Cas9.F^{50} at the indicated MOIs. At three days post-transduction, genomic DNA-derived amplicons covering both RGN target sites were subjected to TE7I-based genotyping assays for determining the frequencies of targeted DSBs in treated populations. In these experiments, cultures of DMD.Δ45–52 myoblasts expressing a non-targeting gRNA (DMD.Δ45–52^{gNEG}), provided for additional negative controls. Open and solid arrowheads indicate the positions of DNA species corresponding to unmodified and RGN-modified sequences, respectively. Lanes M, GeneRuler DNA Ladder Mix; MOI, multiplicity of infection; UN, undetected.

Figure S11B). Moreover, AdV$^{\Delta 2}$P.Cas9.F^{50}-induced targeted DSB formation was also detected at each target site in DMD.Δ45–52 myoblasts co-expressing both gRNAs (DMD.Δ45–52$^{gI52/gI53}$). This finding indicates that AdV-mediated RGN multiplexing is feasible in DMD myoblasts (Supplementary Figure S11B). Importantly, a PCR assay (Figure 6A) showed that exposing DMD.Δ45–52$^{gI52/gI53}$ myoblasts to AdV$^{\Delta 2}$P.Cas9.F^{50} triggered coordinated DSB formation by gI52:Cas9 and gI53:Cas9 complexes leading to the subsequent excision of the intervening 1,123 bp DNA segment encompassing exon 53 (Figure 6B). In contrast, targeted exon 53 deletion events were not detected in experimental conditions lacking one or more elements of this tripartite gene editing system (Figure 6B). Sanger sequencing established that a high proportion of chromosomal DNA junctions formed through AdV-mediated RGN multiplexing were derived from accurate end-to-end joining of distal DSBs (Figure 6C). Clearly, with this strategy, even the fraction of gene-edited cells containing indels at the newly formed intron-intron DNA borders should result in the assembly of precise templates at the mRNA level. Indeed, RT-PCR analysis carried out on differentiated DMD.Δ45–52$^{gI52/gI53}$ myoblasts, initially transduced with AdV$^{\Delta 2}$P.Cas9.F^{50}, gave rise to a single new type of mRNA species whose size difference from unedited templates and nucleotide sequence composition corresponded exactly to in-frame transcripts lacking exon 53 (Figure 6D). Consistent with the data on the characterization of *DMD* editing events at the DNA level (Figure 6B), the detection of corrected mRNA templates was strictly dependent on RGN multiplexing since neither mock-transduced DMD.Δ45–52$^{gI52/gI53}$ myoblasts nor AdV$^{\Delta 2}$P.Cas9.F^{50}-transduced DMD.Δ45–52^{gI53} myoblasts gave rise to myotube populations containing these molecules (Figure 6D).

AdV-mediated *DMD* repair based on long-range targeted DNA deletions

To complement the previous experiments, we next sought to investigate the suitability of AdV delivery of designer nucleases for long-range intragenic deletions involving the major *DMD* mutational hotspot. In these experiments, we have also used the AdV platform to test a hybrid designer nuclease multiplexing strategy in which RGNs and TALENs are

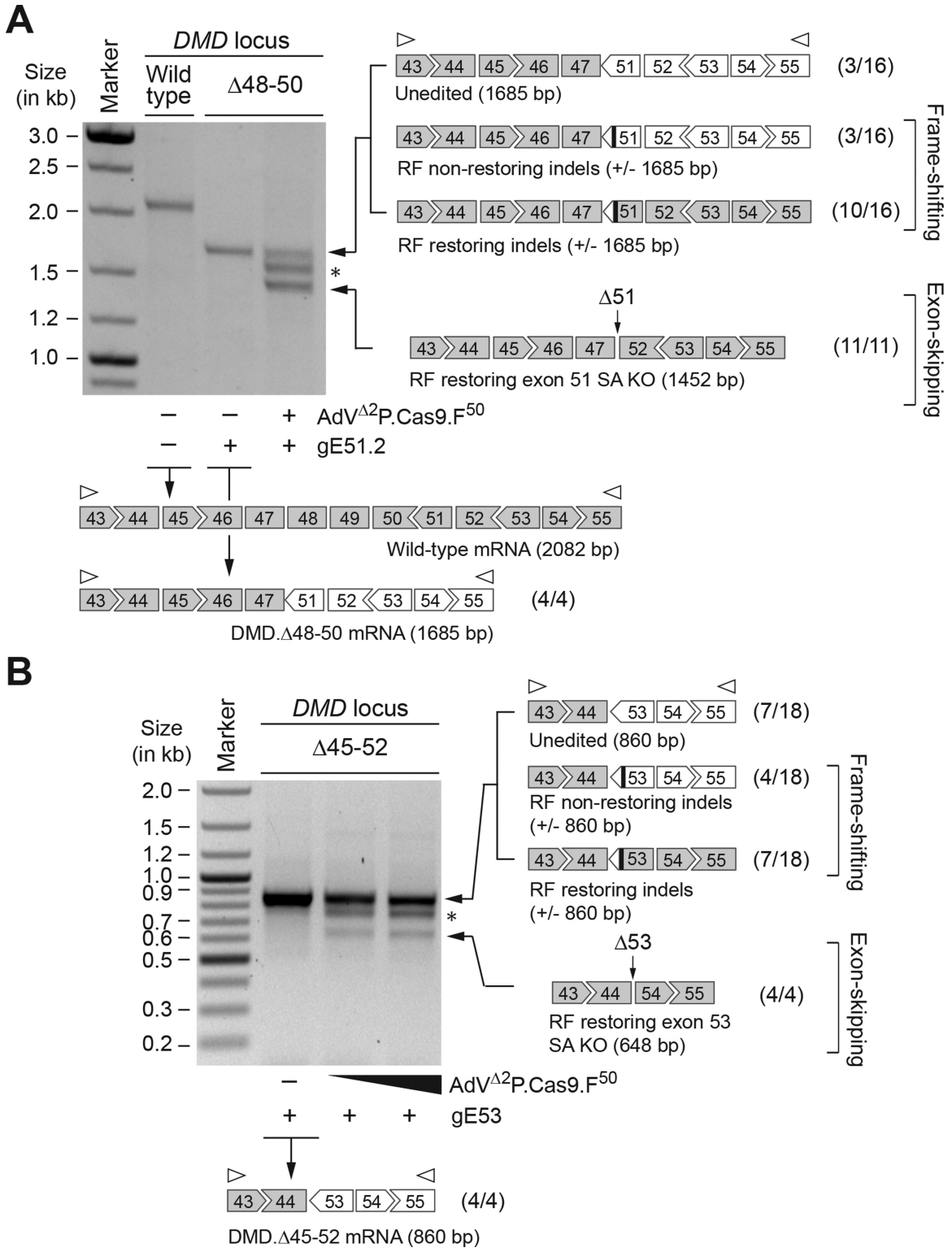

Figure 4. *DMD* transcript repair by NHEJ-mediated indel formation in human myoblasts transduced with Cas9-encoding AdV particles. (**A**) *DMD* reading frame restoration via RGN complexes targeting exon 51. RT-PCR analysis of *DMD* transcripts in myotubes differentiated from healthy donor myoblasts and from patient-derived DMD.Δ48–50$^{gE51.2}$ myoblasts that were either not transduced or transduced with AdV$^{\Delta 2}$P.Cas9.F^{50} at an MOI of 50 IU/cell. (**B**) *DMD* reading frame restoration via RGN complexes targeting exon 53. RT-PCR analysis of *DMD* transcripts in myotubes differentiated from patient-derived DMD.Δ45–52^{gE53} myoblasts that were either not transduced or were transduced with AdV$^{\Delta 2}$P.Cas9.F^{50} at an MOI of 50 and 75 IU/cell. In both panels, arrows indicate the sizes, positions and structures of the different types of *DMD* transcripts identified. The identity and structure of these mRNA molecules was confirmed by cloning and sequencing independent nucleic acid templates whose numbers are specified (digits between brackets). In-frame and out-of-frame sequences are labelled in grey and white, respectively. Vertical bars mark the position of RGN-induced indels. RF, reading frame; SA KO, splice acceptor knockout. Open arrowheads, primers. Marker, GeneRuler DNA Ladder Mix. The asterisks indicate the position of the heteroduplex species formed during PCR by the hybridization of the upper and lower DNA fragments (Supplementary Figure S10).

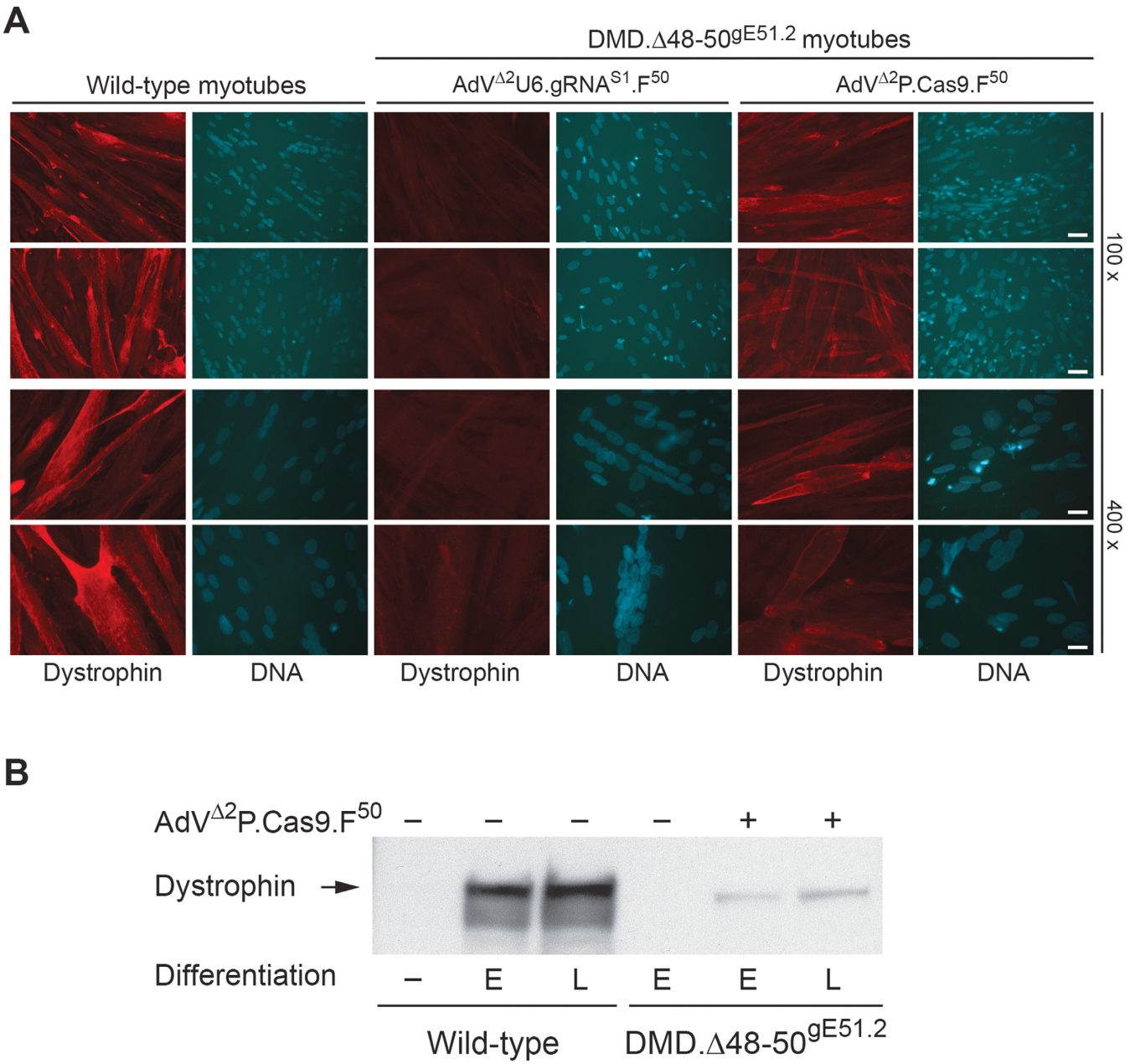

Figure 5. Rescue of dystrophin synthesis by NHEJ-mediated indel formation after AdV delivery of Cas9 nuclease into DMD myoblasts. (**A**) Dystrophin immunofluorescence microscopy on differentiated wild-type and gE51.2-positive DMD.Δ48–50 myoblasts (DMD.Δ48–50$^{gE51.2}$). The dystrophin-defective myoblasts were transduced with negative control vector AdV$^{\Delta 2}$U6.gRNA^{S1}.F^{50} or with Cas9-encoding vector AdV$^{\Delta 2}$P.Cas9.F^{50} at an MOI of 50 IU/cell each. At three days post-transduction, differentiation was triggered by adding mitogen-poor medium with the staining for protein and DNA being performed 5 days later with the aid of an antibody specific for the C-terminus of dystrophin and DAPI, respectively. The horizontal bars in the two upper pictures of the last column correspond to 200 μm; the horizontal bars in the two lower pictures of the last column correspond to 50 μm. (**B**) Dystrophin western blot analysis. Western blotting carried out on myotubes differentiated from DMD.Δ48–50$^{gE51.2}$ myoblasts transduced with AdV$^{\Delta 2}$P.Cas9.F^{50} at an MOI of 50 IU/cell. Myotubes differentiated from healthy donor myoblasts (wild-type) and from mock-transduced DMD.Δ48–50$^{gE51.2}$ myoblasts served as positive and negative controls, respectively. E and L correspond to samples harvested at earlier and later stages of myogenic differentiation. The former and latter stages correspond to cultures containing mostly small and large myotubes, respectively.

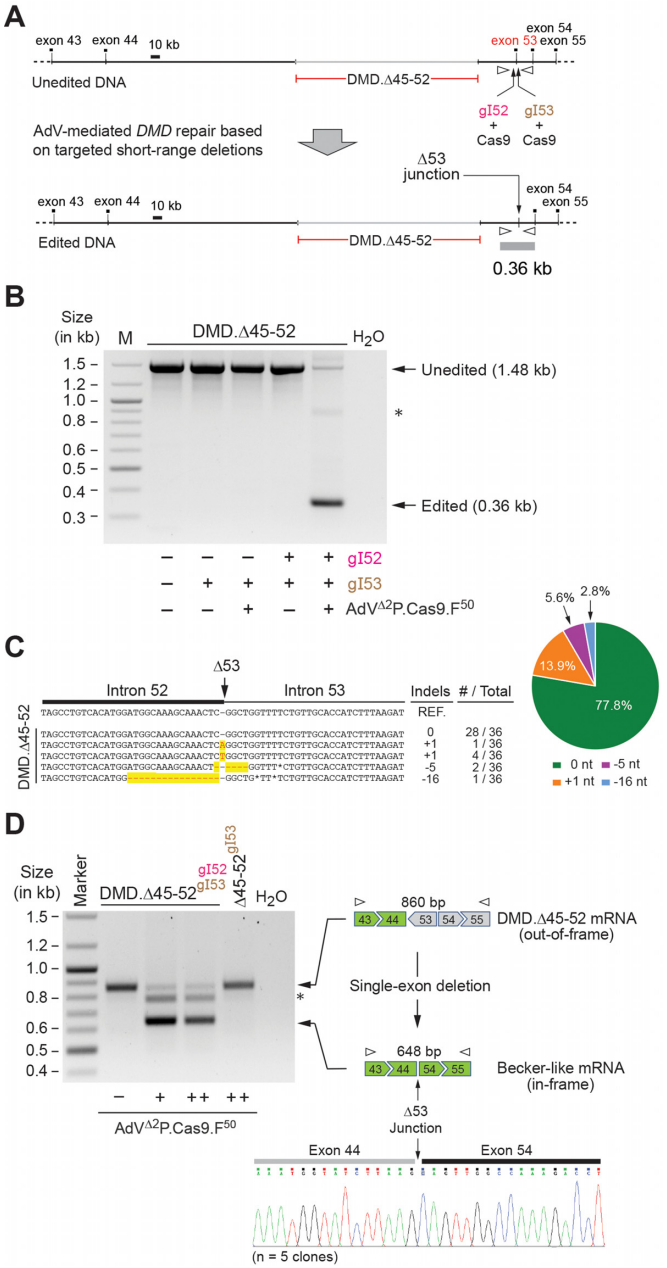

Figure 6. Gene editing based on AdV delivery and RGN multiplexing for NHEJ-mediated short-range *DMD* deletions. (**A**) Schematics of the AdV-mediated *DMD* repair approach based on targeted exon 53 deletion by RGN multiplexing. Concomitant generation of DSBs at *DMD* intron 52 and intron 53 by, respectively, gI52:Cas9 and gI53:Cas9 complexes leads to the removal of the intervening sequence encompassing exon 53 (Δ53). Subsequent NHEJ-mediated joining of the resulting chromosomal termini yield in-frame *DMD* transcripts coding for a Becker-like dystrophin in target cells with a Δ45–53 genotype. These gene editing events can be monitored by PCR with primers specific for sequences present in intron 52 and intron 53 (open arrowheads). (**B**) PCR detection of *DMD* exon 53 deletions generated by AdV-mediated RGN multiplexing. Myoblasts DMD.Δ45–52 expressing gRNA pair gI52/gI53 were transduced with $AdV^{\Delta 2}$P.Cas9.F^{50} at an MOI of 75 IU/cell. At three days post-transduction, genomic DNA was isolated and PCR amplifications was carried out by deploying the primer pair depicted in panel (A). Negative controls consisted of using nuclease-free water and genomic DNA templates extracted from DMD.Δ45–52 myoblasts lacking one or more components of the tripartite gene editing system as indicated. Arrows point to the sizes and positions of PCR products derived from unmodified and edited, Δ53, alleles. The asterisk indicates the positions of the heteroduplex species formed during PCR by the hybridization of the upper and lower DNA fragments. Lanes M, GeneRuler DNA Ladder Mix. (**C**) DNA sequencing analysis of *DMD* junctions assembled by AdV-mediated RGN multiplexing. Sanger sequencing of cloned PCR products representing Δ53 junctions established a high frequency of precise end-to-end joining of chromosomal breaks induced by RGN multiplexing (green slice). (**D**) *DMD* transcript repair in human myoblasts after AdV delivery of RGNs and single-exon deletion. RT-PCR analysis of differentiated DMD.Δ45–$52^{gI52/gI53}$ myoblasts that were either mock-transduced or transduced with $AdV^{\Delta 2}$P.Cas9.F^{50} at MOIs of 50 IU/cell and 75 IU/cell. Differentiated DMD.Δ45–52^{gI52} myoblasts transduced with $AdV^{\Delta 2}$P.Cas9.F^{50} at an MOI of 75 IU/cell served as an extra negative control. Arrows indicate the sizes, positions and structures of the different types of *DMD* transcripts identified. The identity and structure of these mRNA molecules were confirmed by cloning and sequencing of independent nucleic acid templates (n=5). In-frame and out-of-frame sequences are labelled in green and grey, respectively. Open arrowheads represent primers. The asterisk indicates the positions of the heteroduplex species formed during PCR by the hybridization of the upper and lower DNA fragments. Marker, GeneRuler DNA Ladder Mix.

combined. To this end, after assessing two TALEN pairs directed at sequences within *DMD* intron 43 (i.e. 12.TALEN-L/12.TALEN-R and 13.TALEN-L/13.TALEN-R) (Supplementary Figure S12), AdVs encoding each of these proteins were produced. RFLA revealed that all TALEN-encoding expression units were packaged intact within purified AdV particles (Supplementary Figure S13). Importantly, transduction experiments in human myoblasts demonstrated high frequencies of targeted DSB formation at each of the target sites (Supplementary Figure S14). The AdV pair AdV.12.TALEN-L.F^{50} and AdV.12.TALEN-R.F^{50} was selected for subsequent gene editing experiments.

To investigate whether removing the major *DMD* mutational hotspot is feasible in patient-derived myoblasts, the gI54.2:Cas9 complex was combined either with the gI43:Cas9 complex or with the TALEN dimer 12.TALEN-L/12.TALEN-R. Of note, the *DMD* intron 43-specific designer nucleases have overlapping target sequences (Figure 7A). The activity of gI54.2:Cas9 and of its partner gI43:Cas9 was evaluated in AdV$^{\Delta 2}$P.Cas9.F^{50}-transduced DMD myoblasts with both genotypes (i.e. Δ45–52 and Δ48–50) expressing each gRNA component individually or together (Supplementary Figure S15A). Analogous to previous results (Supplementary Figure S11), coordinated DSB formation could be readily detected in AdV$^{\Delta 2}$P.Cas9.F^{50}-transduced cells expressing two gRNAs (Supplementary Figure S15B), opening up for the assessment of long-range excision of the intervening sequence. These *DMD* editing experiments involved co-transducing DMD.Δ45–52$^{gI54.2}$ and DMD.Δ48–50$^{gI54.2}$ myoblasts with AdV$^{\Delta 2}$P.Cas9.F^{50}, AdV.12.TALEN-L.F^{50} and AdV.12.TALEN-R.F^{50} or transducing DMD.Δ45–52$^{gI43/gI54.2}$ and DMD.Δ48–50$^{gI43/gI54.2}$ myoblasts with AdV$^{\Delta 2}$P.Cas9.F^{50}. A PCR assay (Figure 7A) analogous to the one used before for the detection of single-exon deletions (Figure 6A), demonstrated the generation of the predicted intron-intron *DMD* junctions exclusively in target cells that underwent through RGN–TALEN or RGN–RGN multiplexing (Figure 7B, upper and lower panels, respectively). Sanger sequencing demonstrated once again that a high proportion of chromosomal DNA junctions formed through AdV-mediated RGN multiplexing were assembled from precise end-to-end joining of distal DSBs (Figure 7C). Finally, consistent with the products of *DMD* editing at the DNA level (Figure 7B), RT-PCR analysis performed on target cells subjected to AdV-mediated TALEN-RGN and RGN-RGN multiplexing led to the detection of a new transcript form in a *DMD* genotype independent manner (Figure 8). Sanger sequencing showed that this new form consisted exclusively of in-frame mRNA molecules formed by splicing involving exon 43 and exon 55 sequences (Figure 8).

Selection-free rescue of dystrophin synthesis in DMD muscle cell populations after co-delivering Cas9 and gRNA expression units in single AdV particles

Previous work from our laboratory showed that efficient RGN-induced chromosomal DSB formation is chiefly dependent on the total amounts of *gRNA* and *Cas9* expression units rather than on a specific ratio between them (23). As corollary, vector designs in which *gRNA* and *Cas9* transgenes are incorporated within single vector particles aid in setting up robust and simpler gene editing protocols. Related to this, we generated fiber-modified AdVs encoding either Cas9 and gE53 (AdV$^{\Delta 2}$P.Cas9.gE53.F^{50}) or Cas9 and gE51.2 (AdV$^{\Delta 2}$P.Cas9.gE51.2.F^{50}). RFLA demonstrated the structural integrity of these viral vector genomes (Supplementary Figure S16). Importantly, transduction of DMD.Δ48–50 and DMD.Δ45–52 myoblasts with, respectively, AdV$^{\Delta 2}$P.Cas9.gE51.2.F^{50} and AdV$^{\Delta 2}$P.Cas9.gE53.F^{50} resulted in robust targeted DSB formation (Supplementary Figure S17) without the concomitant detection of DSBs at candidate off-target sites (Supplementary Figure S18). Indeed, indel frequencies were similar to those reached in the *DMD*-editing screening systems based on exposing *gRNA*-modified DMD myoblast lines to AdV$^{\Delta 2}$P.Cas9.F^{50}. To confirm that RGN complex assembly is not limiting in target cells transduced with the 'all-in-one' AdV format, we carried out Tracking of Indels by DEcomposition (TIDE) analysis in DMD.Δ45–52^{gE53} myoblasts and in naïve DMD.Δ45–52 parental cells that had been exposed to 100 IU/cell of AdV$^{\Delta 2}$P.Cas9.F^{50} and AdV$^{\Delta 2}$P.Cas9.gE53.F^{50}, respectively. In addition to determining the total efficiency of targeted DSB formation, the TIDE assay provides information on the frequencies of the various types of indels that are generated. The TIDE data revealed that the two experimental settings yielded comparable levels of site-specific DSBs. Notably, the most frequent type of indel identified (i.e. +1) corresponds to *DMD* editing events resulting in in-frame transcripts (Supplementary Figure S19A and S19B). Applying the TIDE assay to naïve DMD.Δ48–50 myoblasts transduced with 100 IU/cell of AdV$^{\Delta 2}$P.Cas9.gE51.2.F^{50} confirmed robust NHEJ-mediated *DMD* repair by using the 'all-in-one' AdV platform (Supplementary Figure S19C).

Subsequently, we investigated the capacity of the 'all-in-one' AdVs to trigger dystrophin protein synthesis in unselected DMD muscle cell populations. To this end, DMD.Δ45–52 and DMD.Δ48–50 myoblasts were induced to differentiate after being transduced with AdV$^{\Delta 2}$P.Cas9.gE53.F^{50} and AdV$^{\Delta 2}$P.Cas9.gE51.2.F^{50}, respectively. Western blot analysis revealed the presence of Becker-like dystrophin molecules exclusively in cultures of DMD myotubes whose progenitors had undergone AdV transductions (Figure 9). In addition, a direct correlation between DSB and *DMD* repair levels could be ascertained in that the most active RGN complex gE51.2:Cas9 (see, for instance, Supplementary Figure S19), led to the highest amounts of *de novo* dystrophin protein synthesis (Figure 9). Finally, we setup a dual-color immunofluorescence microscopy assay (Supplementary Figure S20) for the simultaneous detection of dystrophin and β-dystroglycan. The latter entity constitutes a key component of a large sarcolemma protein complex called the dystrophin-associated glycoprotein complex (DGC). Through its association with the cysteine-rich domain located near the C-terminus of dystrophin, β-dystroglycan is stabilized and properly assembled at the plasma membrane of differentiated muscle cells within the context of the whole DGC. Hence, in the absence of dystrophin/β-dystroglycan linkages, the integrity of the DGC is disrupted.

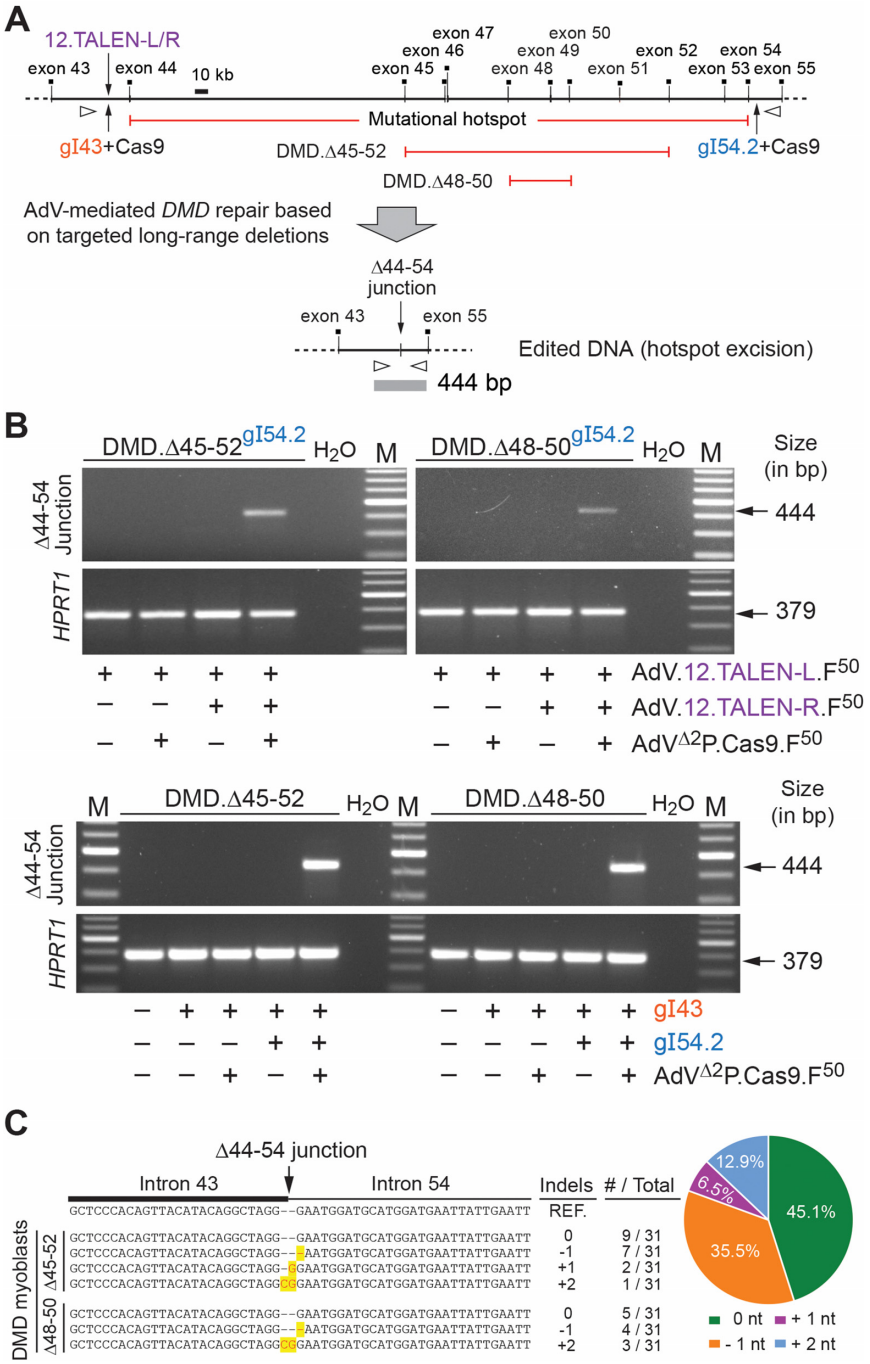

Figure 7. Gene editing based on AdV delivery and designer nuclease multiplexing for NHEJ-mediated long-range *DMD* deletions. (**A**) Schematics of the AdV-mediated *DMD* repair approaches based on targeted deletion of the *DMD* mutational hotspot. Simultaneous generation of DSBs at *DMD* intron 43 and intron 54 by, respectively, gI43:Cas9 and gI54.2:Cas9 complexes lead to the excision of the intervening sequence encompassing exon 44 through exon 54 (Δ44–54). Subsequent NHEJ-mediated joining of the resulting chromosomal termini result in the generation of in-frame *DMD* transcripts coding for a Becker-like dystrophin regardless of whether the target cells have a Δ45–52 or Δ48–50 genotype. The alternative hybrid multiplexing strategy based on combining TALEN dimers 12.TALEN-L/12.TALEN-R with RGN complexes gI54.2:Cas9 yield the same outcome. These gene editing events can be monitored by PCR with primers specific for sequences located in intron 43 and intron 54 (open arrowheads). (**B**) PCR detection of *DMD* mutational hotspot deletions generated by AdV-mediated designer nuclease multiplexing. Myoblasts DMD.Δ45–52 expressing gRNA gI54.2 (DMD.Δ45–52$^{gI54.2}$) were co-transduced with a 1:1:1 mixture of AdV.12.TALEN-L.F50, AdV.12.TALEN-R.F50 and AdV$^{\Delta 2}$P.Cas9.F^{50} at a total MOI of 25 IU/cell (upper panel). Myoblasts DMD.Δ45–52 and DMD.Δ48–50 expressing gRNA pair gI43/gI54.2 were transduced with AdV$^{\Delta 2}$P.Cas9.F^{50} at an MOI of 75 IU/cell (lower panel). Three days later, chromosomal DNA was isolated and subjected to PCR amplifications with the primers shown in panel (A). Negative controls consisted of using nuclease-free water and genomic DNA templates isolated from patient-derived myoblasts lacking one or more components of the tripartite gene editing system as indicated. Arrows mark the sizes and positions of amplicons representing Δ44–54 junctions and internal control *HPRT1* target sequences. Lanes M, GeneRuler DNA Ladder Mix. (**C**) DNA sequencing analysis of *DMD* junctions assembled by AdV-mediated RGN multiplexing. Sanger sequencing of cloned PCR products representing Δ44–54 junctions showed a high frequency of accurate end-to-end NHEJ ligation of chromosomal breaks induced by RGN multiplexing (green slice).

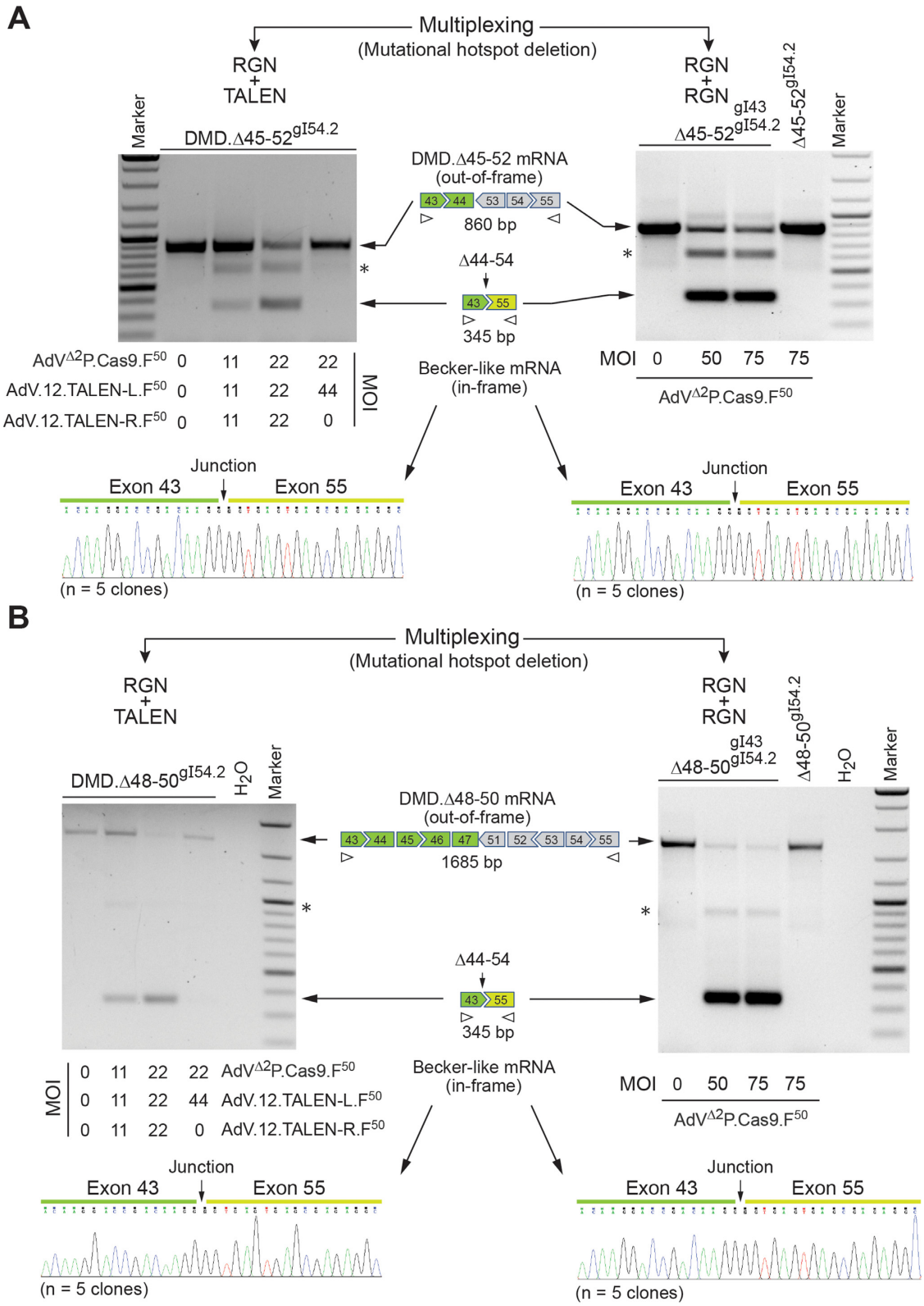

Figure 8. *DMD* transcript repair in human myoblasts after AdV delivery of designer nucleases and long-range DNA deletions. RT-PCR analysis on (**A**) DMD.Δ45–52 myotubes and (**B**) DMD.Δ48–50 myotubes expressing the indicated gRNAs. The progenitors of these myotubes were either mock-transduced or were transduced with the indicated combinations and doses of AdVs encoding Cas9 or TALENs. Arrows indicate the sizes, positions and structures of the various types of *DMD* transcripts identified. The identity and structure of these mRNA molecules were confirmed by cloning and sequencing of independent nucleic acid templates derived from cells transduced at the highest AdV MOIs (n=5). In-frame and out-of-frame sequences are labelled in green and grey, respectively. Open arrowheads represent primers. The asterisk indicate the positions of the heteroduplex species formed during PCR by the hybridization of the upper and lower DNA fragments. MOI, multiplicity of infection. Marker, GeneRuler DNA Ladder Mix.

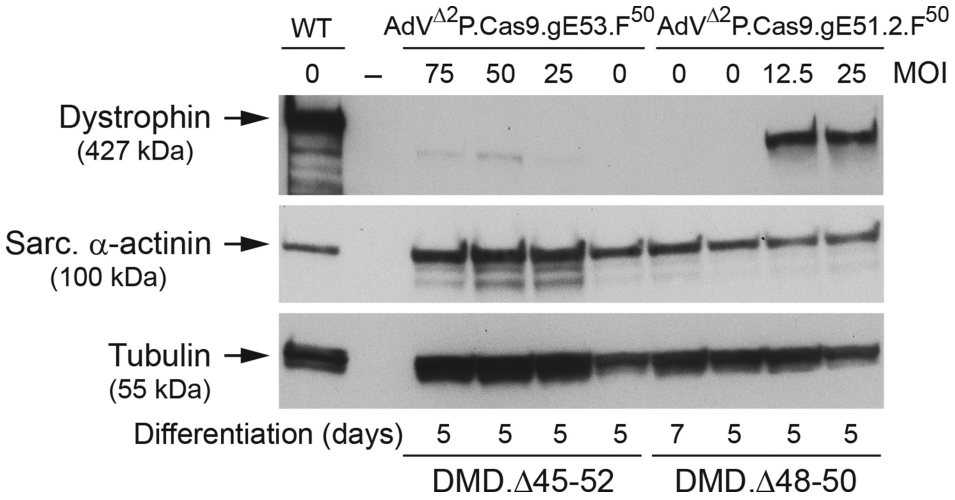

Figure 9. Dystrophin western blotting on myotubes differentiated from DMD myoblasts transduced with RGN-encoding AdVs. DMD.Δ45–52 and DMD.Δ48–50 myoblasts were transduced with AdV$^{\Delta 2}$P.Cas9.gE53.F^{50} and AdV$^{\Delta 2}$P.Cas9.gE51.2.F^{50}, respectively, at the indicated multiplies of infection (MOI). Myotubes derived from healthy donor myoblasts served as the positive control (WT). Negative controls consisted of parallel cultures of myotubes differentiated from mock-transduced DMD myoblasts. After the indicated periods in differentiation medium, western blot analysis was carried out for the detection of dystrophin, sarcomeric α-actinin and tubulin.

Notably, dual-color immunofluorescence microscopy led to the detection of dystrophin in myotubes differentiated from AdV$^{\Delta 2}$P.Cas9.gE51.2.F^{50}-treated DMD.Δ48–50 myoblasts (Figure 10). Significantly, besides no evidence for dystrophin protein synthesis above background levels in DMD.Δ48–50 myotubes, the β-dystroglycan-specific fluorescence was weaker in these syncytia when compared to that found in their AdV-edited counterparts (Figure 10). Indeed, the merging of dystrophin- and β-dystroglycan-specific signals revealed the co-localization of both target proteins in AdV$^{\Delta 2}$P.Cas9.gE51.2.F^{50}-treated cultures. These data indicate that the levels of *de novo* dystrophin synthesis resulting from AdV-mediated *DMD* editing contributed to the stabilization and proper assembly of the DGC.

Taken our data together, we conclude that AdV transduction of designer nucleases offers a versatile and powerful range of strategies for restoring the *DMD* reading frame in dystrophin-defective human muscle progenitor cells warranting, as a result, further investigation.

DISCUSSION

The impact of AdVs on biomedical research is growing. This is exemplified by their testing as recombinant vaccines and as oncolytic agents in an increasing number of clinical trials (41,42). AdVs have also started to be investigated as a source of exogenous DNA templates for homology-directed gene targeting (24,43,44) and/or designer nuclease expression (14,22–24,44). In fact, as a potential AIDS therapy, the *ex vivo* delivery of *CCR5*-specific ZFNs into CD4$^+$ T cells by AdV particles provides the first example of translational genome editing (45). *Ex vivo* gene editing approaches are especially appealing in that contact between the patient and the immunogenic components of vectors and nucleases, are minimized. This is particularly important while using AdVs since their well-established high immunogenic profiles are likely to trigger the elimination of gene-edited cells if applied *in vivo* (46,47). In addition, possible vector re-administrations will possibly be curtailed due to the development of anti-vector neutralizing antibodies. Related to these issues, a recent study provided evidence for Cas9-specific immune responses after AdV transduction of murine livers (48). Notwithstanding the above, while this work was under review, a study by Xu and coworkers based on local intramuscular injection of a first-generation AdV into dystrophic *mdx* mice showed efficient RGN-induced deletion of a 23-kb genomic fragment encompassing the *mdx* point mutation (49). These data adds further support to the potency of these vehicles as gene editing tools.

Previous work from our laboratory has shown that AdVs, in particular fiber-modified AdVs, are able to introduce functional TALEN and Cas9 nucleases into hard-to-transfect, CAR-negative, target cells, including *bona fide* muscle progenitor cells and non-muscle cells with myogenic capacity (22,23). By building on these data and on those of others (9–12), here we have demonstrated that these gene delivery vehicles can be tailored for NHEJ-mediated rescue of *DMD* expression in human myoblasts harboring the most frequent type of *DMD*-causing mutations, i.e., deletions (4). These AdV-based *DMD* editing strategies consisted of expressing one or two designer nuclease complexes in dystrophin-defective human myoblasts. The former involved generating indels at exonic sequences and splicing signals for reading frame resetting and DNA-level exon skipping, respectively; the latter comprised inducing specific exon excisions for in-frame mRNA assembly. In addition, we have also used the AdV platform to achieve a first proof-of-principle for hybrid designer nuclease multiplexing strategies. In particular, we have established that staggered and blunt-ended DSBs generated by TALENs and RGNs, respectively, can yield targeted chromosomal DNA deletions. In addition to the high specificity profile offered by TALENs, the combinatorial use of different designer nu-

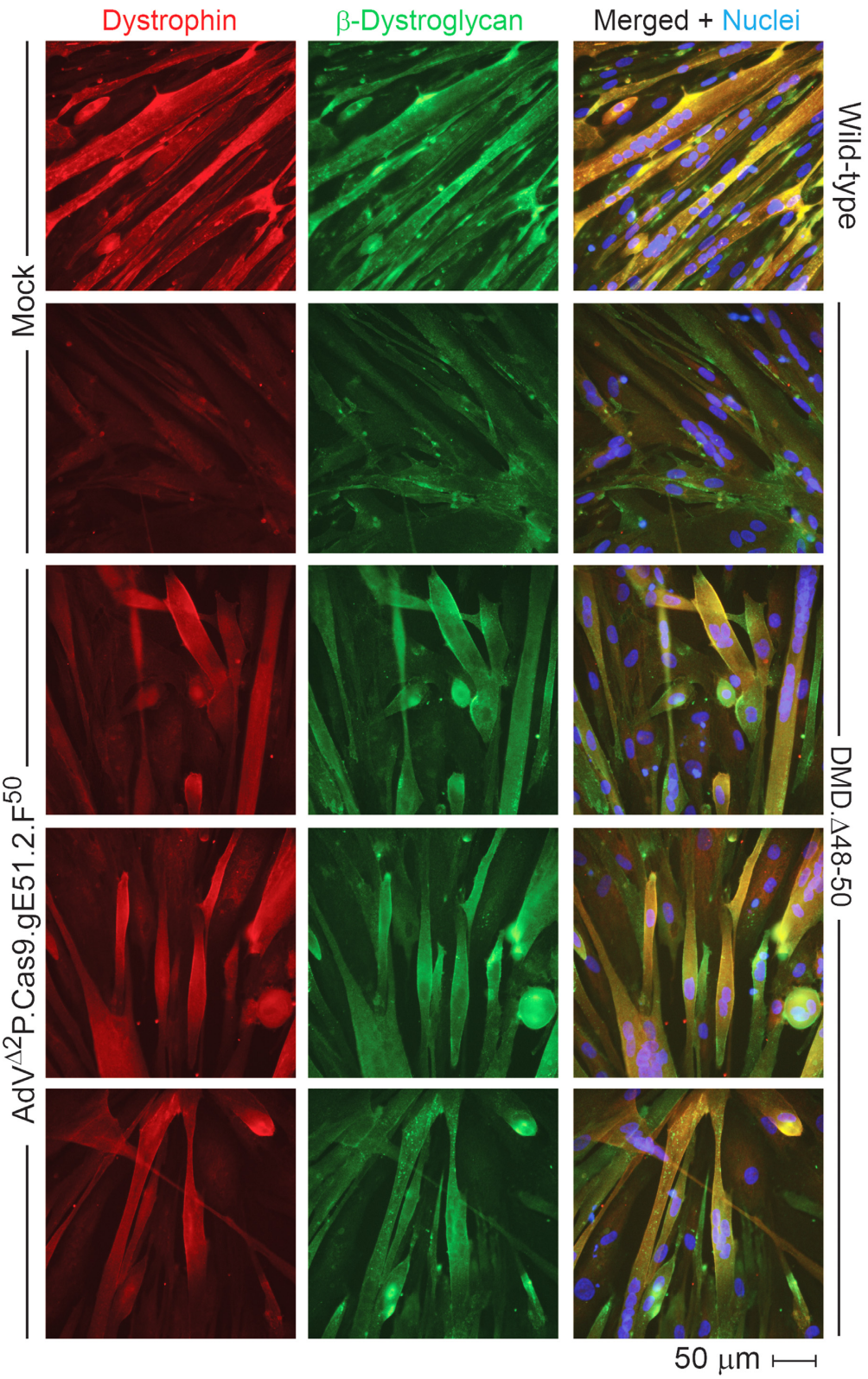

Figure 10. Dystrophin and β-dystroglycan immunofluorescence microscopy on *DMD*-edited myotubes. Immunostainings for dystrophin and β-dystroglycan was carried out in myotubes differentiated from DMD.Δ48–50 myoblasts transduced with AdV$^{\Delta 2}$P.Cas9.gE51.2.F^{50}. Human myotubes derived from a healthy donor (wild-type) and mock-transduced DMD.Δ48–50 myoblasts served as positive and negative controls, respectively.

clease platforms adds yet another level of flexibility to gene editing based on multiplexing.

Clearly, as discussed next, each of these approaches display their own sets of pros and cons. The process of indel-derived frame shifting is stochastic in nature with only a fraction of events resulting in proper reading frame resetting and with some of the resulting products possibly harboring immunogenic epitopes. On the other hand, indel-derived exon skipping might suffer from a high context dependency, i.e., availability of suitable designer nuclease target sites in close proximity to key splicing elements (e.g. SA and exonic splicing enhancer elements). In this regard, Sanger sequencing of molecular clones representing independent gene editing events revealed that a 8-bp 'buffer' sequence located between site-specific DSBs and a SA suffices to prevent frequent knockout of the latter motif even when deploying highly active RGN complexes, e.g. gE51.2:Cas9. This data was confirmed by TIDE analysis of indel distributions in whole target cell populations. Therefore, the fact that targeted DSB-induced exon skipping can be triggered independently of significant AG motif disruption has implications for designing, possibly in a more flexible manner, improved DNA-level exon skipping approaches. These might include the testing of orthogonal or engineered Cas9 variants whose PAM requirements expand the range of gRNA targeting to AT-rich regions characteristic of 3′ intronic splicing motifs (50).

In contrast, despite their higher complexity, RGN-RGN and RGN-TALEN multiplexing approaches offer a higher target-site selection flexibility in that they dependent on DSB formation within normally extensive introns. In addition, besides generating well-defined mRNA transcripts, designer nuclease multiplexing has, in its mutational hotspot excision format, the potential of addressing a wide range of DMD-causing genotypes. However, although off-target chromosomal DNA cleavage is an issue pervading the entire genome editing field, it is naturally most problematic in the case of multiplexing approaches as these increase the risk for adverse genome-modifying events such as ectopic mutagenesis and long-range translocations (14). Indeed, despite the fact that, in the case of male DMD patient cells, there is no duplication in the number of target sequences, the generation of coordinated DSBs within single-copy *DMD* alleles can still trigger non-allelic translocations involving *DMD*-specific and off-target DSBs (14). Hence, future research should include genome-wide monitoring of changes to the genetic make-up of human primary cells exposed to single or multiple designer nucleases. This research will depend on improved bioinformatics tools and on the application of more sensitive and unbiased DSB detection assays (51,52).

In conclusion, the current work demonstrates the utility and versatility of using AdV-mediated delivery of gene editing tools for repairing endogenous *DMD* alleles in human myogenic cells by using a range of targeted DNA manipulations. Such research seeks to address one of the major bottlenecks concerning the testing and application of gene editing principles to human muscle cells, that is, the delivery of designer nucleases. In particular, we have shown that tropism-modified AdVs and designer nuclease technologies can be tailored for rescuing *DMD* expression in human muscle cell populations differentiated from CAR-negative DMD myoblasts and, in doing so, bypass the need for clonal selection of gene-edited cells or enrichment steps for isolating cell fractions exposed to nuclease activity. Related to this, there is a steady amount of work being carried out worldwide on the isolation, characterization and testing of human myogenic cells of muscle and non-muscle origins for cell therapy purposes. These cell types should constitute natural targets for testing *ex vivo* gene editing concepts aiming at tackling muscular dystrophies such as those investigated in the present work. Finally, research on AdV-mediated gene editing might also be worth pursuing in the context of other genetic disorders including those caused by a pathologic gain-of-function or aberrant splicing.

SUPPLEMENTARY DATA

Supplementary Data are available at NAR Online.

ACKNOWLEDGEMENTS

This work is dedicated to the memory of Professor Dirk W. van Bekkum. The authors thank Kamel Mamchaoui (Sorbonne Universite´s, Center for Research in Myology, Paris, France) for the human myoblasts with wild-type and *DMD* exon deletion genotypes. We also thank Joop Wiegnant for his technical assistance with the immunofluorescence microscopy, Anna Gram for providing us with the Blast::EGFP construct and Rob Hoeben for his critical reading of the manuscript (all from the Department of Molecular Cell Biology, Leiden University Medical Center, Leiden, The Netherlands).

FUNDING

Dutch Prinses Beatrix Spierfonds [W.OR11–18]; French AFMTéléthon [grant number 16621]. Xiaoyu Chen is the recipient of a Ph.D. research grant from the China Scholarship Council-Leiden University Joint Scholarship Programme. Luca Stefanucci was the recipient of a European Community's ERASMUS Programme grant. Funding for open access charge: Prinses Beatrix Spierfonds [W.OR11–18].

Conflict of interest statement. None declared.

REFERENCES

1. Hoffman,E.P., Brown,R.H. Jr and Kunkel,L.M. (1987) Dystrophin: the protein product of the Duchenne muscular dystrophy locus. *Cell*, **51**, 919–928.
2. Guiraud,S., Aartsma-Rus,A., Vieira,N.M., Davies,K.E., van Ommen,G.J. and Kunkel,L.M. (2015) The Pathogenesis and Therapy of Muscular Dystrophies. *Annu. Rev. Genomics Hum. Genet.*, Epub ahead of print.
3. Goyenvalle,A., Seto,J.T., Davies,K.E. and Chamberlain,J. (2011) Therapeutic approaches to muscular dystrophy. *Hum. Mol. Genet.*, **20**, R69–R78.
4. Bladen,C.L., Salgado,D., Monges,S., Foncuberta,M.E., Kekou,K., Kosma,K., Dawkins,H., Lamont,L., Roy,A.J., Chamova,T. *et al.* (2015) The TREAT-NMD DMD Global Database: analysis of more than 7, 000 Duchenne muscular dystrophy mutations. *Hum. Mutat.*, **36**, 395–402.
5. Cirak,S., Arechavala-Gomeza,V., Guglieri,M., Feng,L., Torelli,S., Anthony,K., Abbs,S., Garralda,M.E., Bourke,J., Wells,D.J. *et al.*

(2011) Exon skipping and dystrophin restoration in patients with Duchenne muscular dystrophy after systemic phosphorodiamidate morpholino oligomer treatment: an open-label, phase 2, dose-escalation study. *Lancet*, **378**, 595–605.
6. Goemans,N.M., Tulinius,M., van den Akker,J.T., Burm,B.E., Ekhart,P.F., Heuvelmans,N., Holling,T., Janson,A.A., Platenburg,G.J., Sipkens,J.A. *et al.* (2011) Systemic administration of PRO051 in Duchenne's muscular dystrophy. *N. Engl. J. Med.*, **364**, 1513–1522. Erratum in: *N. Engl. J. Med.* (2011), **365**, 1361.
7. Echigoya,Y. and Yokota,T. (2014) Skipping multiple exons of dystrophin transcripts using cocktail antisense oligonucleotides. *Nucleic Acids Ther.*, **24**, 57–68.
8. Popplewell,L., Koo,T., Leclerc,X., Duclert,A., Mamchaoui,K., Gouble,A., Mouly,V., Voit,T., Pâques,F., Cédrone,F. *et al.* (2013) Gene correction of a duchenne muscular dystrophy mutation by meganuclease-enhanced exon knock-in. *Hum. Gene Ther.*, **24**, 692–701.
9. Ousterout,D.G., Perez-Pinera,P., Thakore,P.I., Kabadi,A.M., Brown,M.T., Qin,X., Fedrigo,O., Mouly,V., Tremblay,J.P. and Gersbach,C.A. (2013) Reading frame correction by targeted genome editing restores dystrophin expression in cells from Duchenne muscular dystrophy patients. *Mol. Ther.*, **21**, 1718–1726. Erratum in: *Mol. Ther.* (2013), **21**, 2130.
10. Li,H.L., Fujimoto,N., Sasakawa,N., Shirai,S., Ohkame,T., Sakuma,T., Tanaka,M., Amano,N., Watanabe,A., Sakurai,H. *et al.* (2015) Precise correction of the dystrophin gene in duchenne muscular dystrophy patient induced pluripotent stem cells by TALEN and CRISPR-Cas9. *Stem Cell Rep.*, **4**, 143–154.
11. Ousterout,D.G., Kabadi,A.M., Thakore,P.I., Perez-Pinera,P., Brown,M.T., Majoros,W.H., Reddy,T.E. and Gersbach,C.A. (2015) Correction of dystrophin expression in cells from duchenne muscular dystrophy patients through genomic excision of exon 51 by zinc finger nucleases. *Mol. Ther.*, **23**, 523–532.
12. Ousterout,D.G., Kabadi,A.M., Thakore,P.I., Majoros,W.H., Reddy,T.E. and Gersbach,C.A. (2015) Multiplex CRISPR/Cas9-based genome editing for correction of dystrophin mutations that cause Duchenne muscular dystrophy. *Nat. Commun.*, **6**, 6244.
13. Gaj,T., Gersbach,C.A. and Barbas,C.F. 3rd (2013) ZFN, TALEN, and CRISPR/Cas-based methods for genome engineering. *Trends Biotechnol.*, **31**, 397–405.
14. Maggio,I. and Gonçalves,M.A. (2015) Genome editing at the crossroads of delivery, specificity, and fidelity. *Trends Biotechnol.*, **33**, 280–291.
15. Jasin,M. and Rothstein,R. (2013) Repair of strand breaks by homologous recombination. *Cold Spring Harb. Perspect. Biol.*, **5**, a012740.
16. Mussolino,C., Alzubi,J., Fine,E.J., Morbitzer,R., Cradick,T.J., Lahaye,T., Bao,G. and Cathomen,T. (2014) TALENs facilitate targeted genome editing in human cells with high specificity and low cytotoxicity. *Nucleic Acids Res.*, **42**, 6762–6773.
17. Doudna,J.A. and Charpentier,E. (2014) Genome editing. The new frontier of genome engineering with CRISPR-Cas9. *Science*, **28**, 1258096.
18. Gonçalves,M.A. and de Vries,A.A. (2006) Adenovirus: from foe to friend. *Rev. Med. Virol.*, **16**, 167–186.
19. Capasso,C., Garofalo,M., Hirvinen,M. and Cerullo,V. (2014) The evolution of adenoviral vectors through genetic and chemical surface modifications. *Viruses*, **6**, 832–855.
20. Gonçalves,M.A., Holkers,M., Cudré-Mauroux,C., van Nierop,G.P., Knaän-Shanzer,S., van der Velde,I., Valerio,D. and de Vries,A.A. (2006) Transduction of myogenic cells by retargeted dual high-capacity hybrid viral vectors: robust dystrophin synthesis in duchenne muscular dystrophy muscle cells. *Mol. Ther.*, **13**, 976–986.
21. Gonçalves,M.A., de Vries,A.A., Holkers,M., van de Watering,M.J., van der Velde,I., van Nierop,G.P., Valerio,D. and Knaän-Shanzer,S. (2006) Human mesenchymal stem cells ectopically expressing full-length dystrophin can complement Duchenne muscular dystrophy myotubes by cell fusion. *Hum. Mol. Genet.*, **15**, 213–221.
22. Holkers,M., Maggio,I., Liu,J., Janssen,J.M., Miselli,F., Mussolino,C., Recchia,A., Cathomen,T. and Gonçalves,M.A. (2013) Differential integrity of TALE nuclease genes following adenoviral and lentiviral vector gene transfer into human cells. *Nucleic Acids Res.*, **41**, e63.
23. Maggio,I., Holkers,M., Liu,J., Janssen,J.M., Chen,X. and Gonçalves,M.A. (2014) Adenoviral vector delivery of RNA-guided CRISPR/Cas9 nuclease complexes induces targeted mutagenesis in a diverse array of human cells. *Sci. Rep.*, **4**, 5105.
24. Holkers,M., Maggio,I., Henriques,S.F., Janssen,J.M., Cathomen,T. and Gonçalves,M.A. (2014) Adenoviral vector DNA for accurate genome editing with engineered nucleases. *Nat. Methods*, **11**, 1051–1057.
25. Fallaux,F.J., Bout,A., van der Velde,I., van den Wollenberg,D.J., Hehir,K.M., Keegan,J., Auger,C., Cramer,S.J., van Ormondt,H., van der Eb,A.J. *et al.* (1998) New helper cells and matched early region 1-deleted adenovirus vectors prevent generation of replication-competent adenoviruses. *Hum. Gene Ther.*, **9**, 1909–1917.
26. Havenga,M.J., Holterman,L., Melis,I., Smits,S., Kaspers,J., Heemskerk,E., van der Vlugt,R., Koldijk,M., Schouten,G.J., Hateboer,G. *et al.* (2008) Serum-free transient protein production system based on adenoviral vector and PER.C6 technology: high yield and preserved bioactivity. *Biotechnol. Bioeng.*, **100**, 273–283.
27. Holkers,M., Cathomen,T. and Gonçalves,M.A. (2014) Construction and characterization of adenoviral vectors for the delivery of TALENs into human cells. *Methods*, **69**, 179–187.
28. Janssen,J.M., Liu,J., Skokan,J., Gonçalves,M.A. and de Vries,A.A. (2013) Development of an AdEasy-based system to produce first- and second-generation adenoviral vectors with tropism for CAR- or CD46-positive cells. *Gene Med.*, **15**, 1–11.
29. Cudré-Mauroux,C., Occhiodoro,T., König,S., Salmon,P., Bernheim,L. and Trono,D. (2003) Lentivector-mediated transfer of Bmi-1 and telomerase in muscle satellite cells yields a duchenne myoblast cell line with long-term genotypic and phenotypic stability. *Hum. Gene Ther.*, **14**, 1525–1533.
30. Mamchaoui,K., Trollet,C., Bigot,A., Negroni,E., Chaouch,S., Wolff,A., Kandalla,P.K., Marie,S., Di Santo,J., St Guily,J.L. *et al.* (2011) Immortalized pathological human myoblasts: towards a universal tool for the study of neuromuscular disorders. *Skelet. Muscle*, **1**, 34.
31. Naito,Y., Hino,K., Bono,H. and Ui-Tei,K. (2015) CRISPRdirect: software for designing CRISPR/Cas guide RNA with reduced off-target sites. *Bioinformatics*, **31**, 1120–1123.
32. Bae,S., Park,J. and Kim,J.S. (2014) Cas-OFFinder: a fast and versatile algorithm that searches for potential off-target sites of Cas9 RNA-guided endonucleases. *Bioinformatics*, **30**, 1473–1475.
33. Sambrook,J.F. and Russell,D.W. (2001) *Molecular Cloning: A Laboratory Manual*, 3rd Ed. Cold Spring Harbor Laboratory Press, NY.
34. Kearns,N.A., Genga,R.M., Enuameh,M.S., Garber,M., Wolfe,S.A. and Maehr,R. (2014) Cas9 effector-mediated regulation of transcription and differentiation in human pluripotent stem cells. *Development*, **141**, 219–223.
35. Mali,P., Yang,L., Esvelt,K.M., Aach,J., Guell,M., DiCarlo,J.E., Norville,J.E. and Church,G.M. (2013) RNA-guided human genome engineering via Cas9. *Science*, **339**, 823–826.
36. van Nierop,G.P., de Vries,A.A., Holkers,M., Vrijsen,K.R. and Gonçalves,M.A. (2009) Stimulation of homology-directed gene targeting at an endogenous human locus by a nicking endonuclease. *Nucleic Acids Res.*, **37**, 5725–5736.
37. Pelascini,L.P. and Gonçalves,M.A. (2014) Lentiviral vectors encoding zinc-finger nucleases specific for the model target locus *HPRT1*. *Methods Mol. Biol.*, **1114**, 181–199.
38. Pelascini,L.P., Janssen,J.M. and Gonçalves,M.A. (2013) Histone deacetylase inhibition activates transgene expression from integration-defective lentiviral vectors in dividing and non-dividing cells. *Hum. Gene Ther.*, **24**, 78–96.
39. Miller,J.C., Holmes,M.C., Wang,J., Guschin,D.Y., Lee,Y.L., Rupniewski,I., Beausejour,C.M., Waite,A.J., Wang,N.S., Kim,K.A. *et al.* (2007) An improved zinc-finger nuclease architecture for highly specific genome editing. *Nat. Biotechnol.*, **25**, 778–785.
40. Brinkman,E.K., Chen,T., Amendola,M. and van Steensel,B. (2014) Easy quantitative assessment of genome editing by sequence trace decomposition. *Nucleic Acids Res.*, **42**, e168.
41. Majhen,D., Calderon,H., Chandra,N., Fajardo,C.A., Rajan,A., Alemany,R. and Custers,J. (2014) Adenovirus-based vaccines for fighting infectious diseases and cancer: progress in the field. *Hum. Gene Ther.*, **25**, 301–317.

42. Russell,S.J., Peng,K.W. and Bell,J.C. (2012) Oncolytic virotherapy. *Nat. Biotechnol.*, **30**, 658–670.
43. Coluccio,A., Miselli,F., Lombardo,A., Marconi,A., Malagoli Tagliazucchi,G., Gonçalves,M.A., Pincelli,C., Maruggi,G., Del Rio,M. *et al.* (2013) Targeted gene addition in human epithelial stem cells by zinc-finger nuclease-mediated homologous recombination. *Mol. Ther.*, **21**, 1695–1704.
44. Chen,X. and Gonçalves,M.A. (2015) Engineered viruses as genome editing devices. *Mol. Ther.* Advance online publication; doi: 10.1038/mt.2015.164.
45. Tebas,P., Stein,D., Tang,W.W., Frank,I., Wang,S.Q., Lee,G., Spratt,S.K., Surosky,R.T., Giedlin,M.A., Nichol,G. *et al.* (2014) Gene editing of CCR5 in autologous CD4 T cells of persons infected with HIV. *N. Engl. J. Med.*, **370**, 901–910.
46. Yang,Y., Haecker,S.E., Su,Q. and Wilson,J.M. (1996) Immunology of gene therapy with adenoviral vectors in mouse skeletal muscle. *Hum. Mol. Genet.*, **5**, 1703–1712.
47. Zoltick,P.W., Chirmule,N., Schnell,M.A., Gao,G.P., Hughes,J.V. and Wilson,J.M. (2001) Biology of E1-deleted adenovirus vectors in nonhuman primate muscle. *J. Virol.*, **75**, 222–5229.
48. Wang,D., Mou,H., Li,S., Li,Y., Hough,S., Tran,K., Li,J., Yin,H., Anderson,D.G., Sontheimer,E.J. *et al.* (2015) Adenovirus-mediated somatic genome editing of *Pten* by CRISPR/Cas9 in mouse liver in spite of Cas9-specific immune responses. *Hum. Gene Ther.*, **26**, 432–442.
49. Xu,L., Park,K.H., Zhao,L., Xu,J., El Refaey,M., Gao,Y., Zhu,H., Ma,J. and Han,R. (2015) CRISPR-mediated genome editing restores dystrophin expression and function in mdx mice. *Mol Ther.*, Doi: 10.1038/mt.2015.192.
50. Esvelt,K.M., Mali,P., Braff,J.L., Moosburner,M., Yaung,S.J. and Church,G.M. (2013) Orthogonal Cas9 proteins for RNA-guided gene regulation and editing. *Nat. Methods*, **10**, 1116–1121.
51. Wu,X., Kriz,A.J. and Sharp,P.A. (2014) Target specificity of the CRISPR-Cas9 system. *Quant. Biol.*, **2**, 59–70.
52. Hendel,A., Fine,E.J., Bao,G. and Porteus,M.H. (2015) Quantifying on- and off-target genome editing. *Trends Biotechnol.*, **33**, 132–140.